Chaperone-Dependent Degradation of Cdc42 Promotes Cell Polarity and Shields the Protein from Aggregation

by Beatriz González[1,a], Martí Aldea[2], and Paul J. Cullen[1] †

[1]Department of Biological Sciences, State University of New York at Buffalo

[2]Molecular Biology Institute of Barcelona (IBMB), CSIC, Barcelona, Spain

[a]Current address: Department of Genetics, Microbiology and Statistics, School of Biology, University of Barcelona, Barcelona, Spain. (beatriz.gonzalez@ub.edu)

Corresponding author: † Paul J. Cullen

532 Cooke Hall

Department of Biological Sciences

State University of New York at Buffalo

Buffalo, NY 14260-1300

Phone: (716)-645-4923

FAX: (716)-645-2975

Email: pjcullen@buffalo.edu

Author Contributions: B.G. designed experiments, generated data and wrote the paper. M.A. designed experiments. P.J.C. designed experiments and wrote the paper.

Running title: Exploring Chaperone-Dependent Degradation of Cdc42

Keywords: temperature, protein trafficking, ESCRT, sexual selection, quality control, protein aggregation, aging, mitogen-activated protein kinases, GTPases, and cell signaling.

Summary statement:

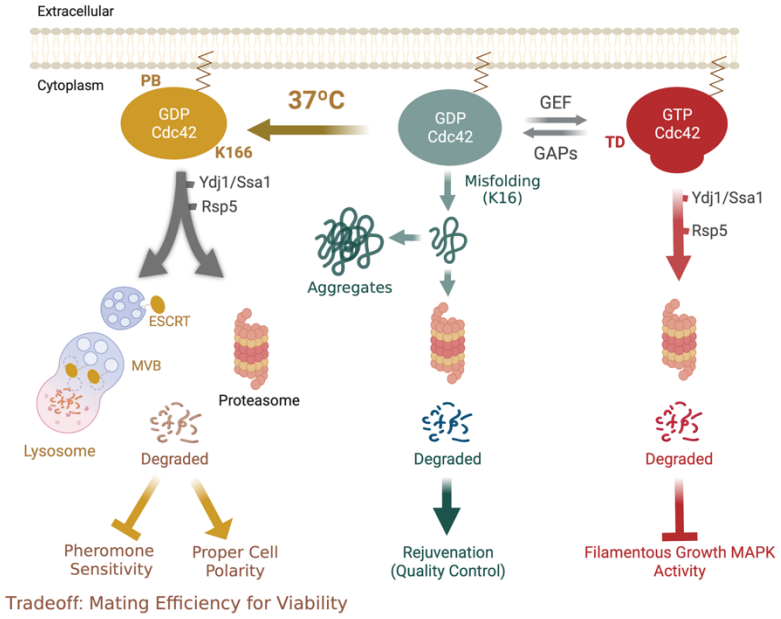

Rho GTPases are global regulators of cell polarity and signaling, and when mis-regulated can cause diseases including cancers. By exploring the turnover regulation of the yeast Rho GTPase Cdc42p, we have identified new regulatory features surrounding the stability of the protein. We specifically show that Cdc42p was degraded at high temperatures (37˚C) in a chaperone-dependent manner by two routes: one required the 26S proteasome and the other occurred in an ESCRT-dependent pathway in the lysosome/vacuole. By analyzing versions of Cdc42p that were defective for turnover, we show that turnover at 37˚C promoted cell polarity but was defective for sensitivity to mating pheromone, presumably mediated through a Cdc42p-dependent MAP kinase pathway. Versions of Cdc42p that were required for the stability of the protein were also identified. Accumulation of mis-folded Cdc42p in certain settings lead to the formation of protein aggregates. Our study uncovers new aspects of Rho GTPase turnover regulation that may extend to other systems. Moreover, several residues identified here that mediate Cdc42p turnover are also found to correlate in with several human diseases, which may suggest that turnover regulation of Cdc42p may be important to aspects of human health.

ABSTRACT

Rho GTPases are global regulators of cell polarity and signaling. By exploring the turnover regulation of the yeast Rho GTPase Cdc42p, we identified new regulatory features surrounding the stability of the protein. We specifically show that Cdc42p is degraded at 37ºC by chaperones through lysine residues located in the C-terminus of the protein. Cdc42p turnover at 37˚C occurred by the 26S proteasome and also in an ESCRT-dependent manner in the lysosome/vacuole. By analyzing versions of Cdc42p that were defective for turnover, we show that turnover at 37˚C promoted cell polarity but was defective for sensitivity to mating pheromone, presumably mediated through a Cdc42p-dependent MAP kinase pathway. We also identified one residue (K16) in the P-loop of the protein that was critical for Cdc42p stability. Accumulation of Cdc42p^{K16R} in some contexts led to the formation of protein aggregates, which were enriched in aging mother cells and cells undergoing proteostatic stress. Our study uncovers new aspects of protein turnover regulation of a Rho-type GTPase that may extend to other systems. Moreover, several residues identified here that mediate Cdc42p turnover are also found to correlate in with several human diseases, which may suggest that turnover regulation of Cdc42p may be important to aspects of human health.

Keywords: Temperature, protein trafficking, ESCRT, sexual selection, tradeoffs, quality control, protein aggregation, aging

INTRODUCTION

Rho (Ras homology) GTPases of the Ras superfamily are global regulators of cytoskeletal dynamics and signal transduction pathways (Etienne-Manneville and Hall, 2002; Ridley, 2011). Rho GTPases function as molecular switches, activated by guanine nucleotide exchange factors (GEFs) that catalyze exchange of GDP for GTP, and inactivated by GTPase activating proteins (GAPs) that promote intrinsic GTP hydrolysis (Bos et al., 2007). The active or GTP-bound state leads to interaction with a wide variety of effector proteins that can modulate the shape and migration of cells, as well as cell cycle progression, gene expression, apoptosis and survival (Coleman et al., 2004; Lawson and Ridley, 2018; Prudnikova et al., 2015).

Rho GTPases are also regulated by post-translational modifications (PTMs), which control the spatiotemporal regulation and activity of Rho GTPases. One type of regulation impacts Rho GTPase stability, which is mainly controlled by ubiquitination (Guo and Rahmouni, 2019; Majolée et al., 2021; Vanneste et al., 2020; Wei et al., 2013).

Moreover, the mis-regulation of Rho GTPase protein levels have begun to be implicated several human diseases including cancers (Clayton and Ridley, 2020; Goka and Lippman, 2015; Haga and Ridley, 2016; Li et al., 2016) and neurodegenerative disorders (Arrazola Sastre et al., 2020). Given that changes to CDC42 activity have been proposed to impact cell migration and invasion during malignant transformation (Reymond et al., 2012; Svensmark and Brakebusch, 2019; Zhang et al., 2019), as well as cellular aging (Florian et al., 2012; Geiger and Zheng, 2013), molecular mechanisms that regulate CDC42 stability might be relevant to human diseases and aging.

Proteins in the cell are turned over after ubiquitination by two major pathways. One pathway requires the 26S proteasome (Amm et al., 2014; Finley et al., 2012), and is the major route for turnover of Rho GTPases. Another pathway involves the delivery of proteins by intracellular trafficking to the lysosome or vacuole in yeast (Settembre et al., 2013; Wang et al., 2018), which requires the Endosomal sorting complexes required for transport (ESCRT). ESCRT functions to internalize proteins from the surface of the endosomes to multivesicular bodies [MVBs, (Katzmann et al., 2001; Remec Pavlin and Hurley, 2020)], and is involved in a wide range of cellular processes, including cytokinesis, neurogenesis, and nuclear envelope regulation (Lu and Drubin, 2020; Vietri et al., 2020; Zhou et al., 2019). The yeast E3 ubiquitin ligase Rsp5p controls the turnover of proteins by the 26S proteasome (Brückner et al., 2011; Fang et al., 2014; Sommer et al., 2014). More commonly, Rsp5p mediates the turnover of plasma membrane proteins in the lysosome or vacuole (Lin et al., 2008; Pizzirusso and Chang, 2004; Rotin et al., 2000; Yoshida et al., 2012). Recently, Rsp5p has been found to mediate the ubiquitination of Heat Shock Proteins (HSP), including Hsp70p-Ssb1p, Hsp82p and Hsp104p in the proteasome (Wang et al., 2021). HSPs are evolutionary conserved molecular chaperones that regulate protein maturation, trafficking, re-folding and degradation (Balchin et al., 2016; Rosenzweig et al., 2019), and accordingly play a critical role in several human diseases (Albakova et al., 2022; Gorenberg and Chandra, 2017; Horianopoulos and Kronstad, 2021).

In the budding yeast *Saccharomyces cerevisiae*, Cdc42p (which is 81% identical to human CDC42) is an essential protein and the principal regulator of cell polarity during budding, mating, and filamentous growth (Bi and Park, 2012; Miller et al., 2020). By interaction with effector proteins, including the formin Bni1p (Evangelista et al., 1997; Evangelista et al., 2002), Gic proteins (Brown et al., 1997; Kawasaki et al., 2003), and p21-activated kinase PAKs (Cvrcková et

al., 1995; Evangelista et al., 2002; Gulli et al., 2000), Cdc42p controls the establishment of cell polarity and the formation of a new bud (Lamas et al., 2020; Martin, 2015; Miller et al., 2020; Moran et al., 2019; Slaughter et al., 2009). Cdc42p binds to Ste20p to regulate Mitogen-Activated Protein Kinase (MAPK) pathways (Cvrcková et al., 1995; Peter et al., 1996; Saito, 2010; Simon et al., 1995). Three Cdc42p-dependent MAPK pathways regulate different cellular responses, including filamentous growth (fMAPK) (Cullen and Sprague, 2012), mating (Good et al., 2009; Ni et al., 2011; Sieber et al., 2022; Sprague et al., 1983), and the response to osmotic stress (HOG) (Saito and Posas, 2012). Cdc42p also regulates exocytosis (Adamo et al., 2001), endocytosis (Aguilar et al., 2006), vacuolar functions (Jones et al., 2010), and nuclear membrane disassembly and migration (Lu and Drubin, 2020). However, many questions about the regulation of Cdc42p stability and its impact on biological functions remain unanswered.

We previously showed that heat shock proteins (HSPs) of the HSP40/HSP70 family direct GTP-bound Cdc42p (called GTP-Cdc42p in this study) to the E3 ubiquitin ligase Rsp5p for turnover in the proteasome (González and Cullen, 2022). This discovery prompted examination of other aspects of Cdc42p turnover. HSPs control protein folding and turnover at high temperatures, which suggested that temperature may play a role in Cdc42p turnover regulation. In line with this possibility, we show here that Cdc42p is also turned over at 37ºC, which required the same HSP40/HSP70 and Rsp5p proteins. We also identified lysine residues specifically required for turnover of Cdc42p at 37˚C. Moreover, whereas GTP-Cdc42p was turned over in the proteasome, at 37˚C, Cdc42p was turned over by the proteasome and in the ESCRT-to-vacuole pathway, which represents the first example for turnover of a Rho-type GTPase in this compartment. Turnover of Cdc42p at 37ºC reduced the sensitivity to mating pheromone (by a MAPK pathway), which indicates that that the turnover of Cdc42p is functionally relevant in this context. Interfering with

Cdc42p turnover at 37˚C restored pheromone sensitivity but also led to defects in viability and cell polarity, suggesting that Cdc42p degradation at 37ºC is required for proper cell function. Finally, we identified one residue (K16) that was critical for the stability of the protein. Accumulation of $Cdc42p^{K16R}$ in the cell (or overproduction of the protein) led to the formation of protein aggregates. Our findings provide new insights into the molecular basis of Cdc42p stability and the functional consequences on biological activities, ranging to sexual selection tradeoffs to aging. These findings may extend to the regulation of Rho GTPases in many settings.

MATERIALS AND METHODS

Yeast strains, reagents and media

All Strains used in this study are listed in Table 1, plasmids in Table 2, and primers in Table 3. Yeast strains were grown in YEPD media [Yeast Extract Peptone Dextrose; 1% bacto-yeast extract, 2% bacto-peptone, 2% dextrose], YEPGAL media (Yeast Extract Peptone Dextrose; 1% bacto-yeast extract, 2% bacto-peptone, 2% galactose) media and SD media (Synthetic Dextrose; 0.67% yeast nitrogen base without amino acids, 2% dextrose) media supplemented with amino acids when required unless otherwise indicated (Rose et al., 1990). Cells were grown at 30ºC or 37ºC, otherwise temperature is indicated in the corresponding figure legend. To maintain the selection of the plasmids, cells were grown in SD media lacking uracil. pRS306-GFP-linker-Cdc42 (pDLB3609) plasmid was kindly provided by the Lew Lab (Woods et al., 2016b). To construct the pGFP-Cdc42 plasmid (PC6454) driven by *CDC42* promoter, pRS306-GFP-linker-CDC42 was subcloned with with *EcoR*I and *Sal*I into pRS316 [CEN/URA (Sikorski and Hieter, 1989)]. To generate the pHis6x-linker-Cdc42 and pHis6x-linker-$Cdc42^{13KR}$ by homologous recombination,

158 pGFP-Cdc42 was linearized with the restriction enzyme SnaBI (Cat#R0130S, New England
159 Biolabs), and co-transformed in yeast with primers harboring the *HISX6* sequence and flanking
160 regions to the *CDC42* promoter and linker, sequences listed in Table 3. Gene disruptions were
161 done according to standard techniques using antibiotic resistance markers NAT, HYG and
162 KanMX6 (Goldstein and McCusker, 1999; Longtine et al., 1998). GeneART™ Site-Directed
163 Mutagenesis (SDM) Kit (Cat#A13282, Thermo Fisher) was used to insert point mutations in the
164 pRS306-GFP-linker-CDC42 plasmid. Other mutations were inserted in the pRS306-GFP-linker-
165 CDC42 plasmid by *in vivo* homologous recombination in yeast. pRS306-GFP-linker-CDC42
166 plasmid was linearized with *PshA*I (Cat#R0593S, New England Biolabs) and co-transformed with
167 a PCR product containing the desired K-to-R changes into an uracil auxotrophic strain (PC538).
168 Positive isolates were confirmed by sequencing.
169
170 ***Protein immunoblot analysis***
171 Cells were grown in YEPD or SD media for 16 h and resuspended into fresh media and grown for
172 4-6 h to mid-log phase or indicated time points. Immunoblotting was performed as described
173 previously (Lee and Dohlman, 2008). Pellets were harvested by centrifugation, washed once in
174 water, and stored at -80ºC. 300µL of trichloroacetic acid buffer (10mM Tris pH 8.0, 25mM
175 NH_4OAc, 1 mM EDTA) made fresh and stored at -20ºC for 5 min was added to precipitate proteins,
176 followed by a mechanical disruption of cells by vortexing for 90 s and place on ice for 60s (3
177 times) with the addition of 50 µL of glass beads. Lysates were centrifugated for 15 min at 4ºC, and
178 resuspended in SDS buffer (0.1M Tris pH 11.0, 5% SDS), boiled for 5 min, and then centrifugated
179 15 s to remove cell debris. The supernatant was diluted 1:1 with 50µM dithiothreitol and 1% of
180 bromophenol blue. Protein extracts were resolved by SDS-PAGE analysis, and proteins were

transferred to ~~a~~ nitrocellulose membranes (Cat#10600003, Amersham™ Protran™ Premium 0.45 µm NC, GE Healthcare Life Sciences), which were incubated in blocking buffer (5% nonfat dry milk, 10mM Tris-HCL [pH 8], 150mM NaCl, and 0.05% Tween 20) for 1 h at room temperature before antibody incubation. Incubations with the primary antibody were carried out at 4ºC during 16h and the secondary antibody at room temperature for 1h. Antibodies were used at the manufacturer's recommended concentrations. Proteins were visualized by Gel Doc XR Imaging System (Bio-Rad, Inc.), after addition of Chemiluminescent HRP substrate for chemiluminescent Westerns (Radiance™ Plus Substrate, Azure Biosystems). Mouse monoclonal antibodies were used to detect green fluorescent protein (GFP) (Cat#11814460001, clones 7.1 and 13.1, Roche). Rabbit polyclonal anti-Cdc42p antibodies are not commercially available and were kindly provided by Dr. Keith Kozminski (Kozminski et al., 2000) (University of Virginia) and used at 1:1,000 dilution. Mouse monoclonal anti-Pgk1p antibodies (22C5D8, Cat#459250, Invitrogen) were used to measure protein levels. Anti-mouse IgG-HRP (Cat# 1706516, Bio-Rad Laboratories) and goat anti-rabbit IgG-HRP (Cat#115-035-003, Jackson ImmnunoResearch Laboratories) secondary antibodies were used. Quantification of band intensity were performed under non-saturated conditions and normalized to the Pgk1p protein using the Image Lab Software (Bio-Rad, Inc.).

Analysis of protein turnover with cycloheximide (CHX) was performed as previously described (Adhikari et al., 2015a). Briefly, 100ml of wild-type cells at 0.02 of O.D. were grown in SD media at 30ºC. After 4h of incubation, the media was supplemented with 25 µg/ml of CHX, and 10 mL of samples were collected at 0, 15, 30, 45, 60, 90 and 120 min to generate cell extracts for immunoblot analysis. Experiments were performed in two biological replicates.

Different strain backgrounds showed different rates of turnover of Cdc42p at 37ºC (S288c showed slower turnover kinetics than Σ1278b, which was focused on here). The difference in turnover rates could be because the strains have different degrees of thermotolerance, although we have not explored this possibility.

Mating Pathway Activity and the Response to Pheromone

Mating pathway activity was evaluated by halo assays (Sprague et al., 1983). Cells were grown for 16 h in SD-URA media, and 200 µL of a 1:100 dilution were spread on SD-URA plates. After the plates were air dried, two concentrations of α-factor, 3 µL (1.8 µM) and 10 µL (6 µM) were applied to the surface. Plates were incubated at 30ºC, 32.5ºC, 34ºC and 36ºC for 2, 3 or 4 days and photographed.

Modeling Protein Structure

To obtain the Cdc42p yeast structure, the protein sequence was overlapped onto the crystal structure of human Cdc42p using the Expasy web server SWISS-MODEL (https://swissmodel.expasy.org) (Nassar et al., 1998).

cBioPortal for Cancer Genomics

The website of cBioPortal for Cancer Genomics (https://www.cbioportal.org) was consulted to look for CDC42 mutations in cancer patients.

Protein localization and fluorescence microscopy

The localization of GFP-Cdc42p (PC6454) and the GFP-Cdc42p alleles where the expression of the fused protein is driven by the *CDC42* promoter. Wild-type and mutant strains were grown in SD media lacking uracil for plasmid selection for 16h at 30ºC, resuspended in fresh media and grown for 4 or 5h to mid-log phase, unless otherwise indicated. To visualize GFP-Cdc42p in the temperature sensitive mutant *cim3-1*, cells were grown for another 2 h at 37ºC.

Differential interference contrast (DIC) and fluorescence microscopy using fluorescein isothiocyanate (FITC) and Rhodamine filter sets were performed using an Axioplan 2 fluorescence microscope (Zeiss) with a Paln-Apochromat 100x/1.4 (oil) objective with the Axiocam MRm camera (Zeiss). Images were analyzed using Axiovision 4.4 software (Zeiss). Staining with the lipophilic dye FM4-64 were performed as described in (Amberg et al., 2006). Images were analyzed with ImageJ (https://imagej.nih.gov) and Adobe Photoshop. Fluorescence images are shown in green (GFP) or red (FM4-64) or converted to grayscale and inverted using ImageJ. Confocal microscopy was performed as previously described (Prabhakar et al., 2020).

Confocal microscopy

Experiments were performed based on (Prabhakar et al., 2020; Prabhakar et al., 2021).The *cim3-1*mutant (PC5852) expressing GFP-Cdc42p (PC6454) or GFP-Cdc42p^{K16R} (PC7697) was grown at 30˚C for 16 h on SD-URA. 10 μL of cells diluted to 0.02 O.D. were placed under 1% agarose pads using a 12 mm Nunc glass base dish (Cat#150680, Thermo Scientific, Waltham). Cells were grown at 30˚C for 3 h prior to imaging. To prevent dehydration, a cotton pad was placed around the agar. Live-cell microscopy was performed with a Zeiss 170 confocal microscope equipped with a Plan-Apochromat 40x/1.4 Oil DIC M27 objective. For the detection of GFP-Cdc42p a 488nm laser (496nm-548nm filter), was used. Images were taken with multiple Z-stacks (8-10)

and a distance of 1 µm between each Z-stack. Images were analyzed with ImageJ using the Z-project and template matching plugins.

Experiments Utilizing the Mother Enrichment Program

Mother Enrichment Program cells (Lindstrom and Gottschling, 2009) (PC7713) expressing GFP-Cdc42p (PC6454) were grown 16 h in SD-URA media supplemented with 0.02 mg/l of adenine. 0.005OD (600nm) of cells were resuspended in 10 ml of fresh SD-URA media supplemented with 0.02 mg/l adenine and 1µM of β-estradiol and grown for 48 h at 30ºC. Cells were collected using a 0.2 µm pore centrifuge filter and a soft spin (1,000 rpm). Cells were washed twice with phosphate-buffered saline solution (PBS; 137 mM NaCl, 2.7 mM KCl, 10 mM Na_2HPO_4, 1.8 mM KH_2PO_4) in the column and stained with 20 µg/ml of WGA-conjugates fluorochrome (Wheat Germ Agglutinin, Alexa Fluor 647 Conjugate; Cat# W32466, Thermo Scientific, Waltham) for 30 min on ice. Cells were washed twice with PBS and resuspended into 50 µL of fresh media prior imaging. Cell microscopy was performed with inverted Leica DMI8 THUNDER microscope equipped with HC PL APO 63x/1.20 W CORR CS2 objective. For the detection of GFP-Cdc42p a 490 nm (BP475-BP515 nm), and for WGA-alexa-647 a 660 nm (BP640-BP720 nm) LED filters were used.

Statistical Analysis

Statistical evaluations were performed with Prism 7 (GraphPad; https://www.graphpad.com/scientific-software/prism/). One-way ANOVA test followed by Tukey's multiple comparison test were used to compare more than two datasets. Mann-Whitney U test non-parametric test was used to analyzed levels of GFP-Cdc42p at the plasma membrane. Tests were indicated for each experiment in the corresponding figure legend.

RESULTS

Cdc42p is Degraded at High Temperatures (37ºC) in an HSP40/HSP70- and Rsp5p-Dependent Manner

Cdc42p protein levels were examined by growth of cells in different environments. Immunoblot analysis using antibodies against the Cdc42p protein showed reduced protein levels during growth at 37˚C (**Figs. 1A**). Immunoblot analysis using anti-GFP antibodies showed that a functional GFP-Cdc42p fusion protein showed a similar pattern (**Fig. 1A**, bottom). Antibodies that recognize the yeast Cdc42p protein and the GFP epitope to detect the GFP-Cdc42p fusion were used interchangeably throughout this study. Cdc42p was not turned over by incubation of cells at 30ºC (**Fig. 1B**; for quantification see **Fig. 1C**). The half-life of the protein was >120 min at 30ºC and reduced < 5min at 37ºC (**Fig. 1C**).

HSP chaperones are upregulated during heat stress to promote protein folding and turnover (Farhan et al., 2021; Lindquist and Craig, 1988). We previously showed that the HSP40-type chaperone Ydj1p (Reidy et al., 2014) is required for turnover of GTP-Cdc42p (González and Cullen, 2022). At 37˚C, Cdc42p levels at 37ºC were also dependent on Ydj1p (**Fig. 1D**). HSP40 proteins function as co-chaperones for HSP70 proteins by controlling the rate of ATP hydrolysis and by directing HSP70s to function in a variety of processes (Craig and Marszalek, 2017). At 37˚C, an HSP70 chaperone, Ssa1p, was also required ~~for~~ to maintain Cdc42p levels (**Fig. 1E**). HSP40 proteins can target client proteins for degradation through the NEDD4-type ubiquitin ligase Rsp5p (Fang et al., 2014). We previously found that poly-ubiquitination of GTP-Cdc42p was dependent on Rsp5p (González and Cullen, 2022). Immunoblot analysis showed that GFP-Cdc42p was also stabilized in the *rsp5-1* mutant at 37ºC (**Fig. 1F**; half-life > 5h), consistent with previous

294 findings (González and Cullen, 2022). Therefore, high temperature (37ºC) is a new stimulus that
295 induces Cdc42p degradation in a HSP40/HSP70- and Rsp5p-dependent manner.

296

297 ***Different lysine residues impact Cdc42p degradation in specific contexts***

298 Ubiquitination involves the covalent modification of lysine residues by E3 ubiquitin ligases
299 (Swatek and Komander, 2016). We previously identified lysine residues required for turnover of
300 GTP-Cdc42p [**Fig. 2A**, K5, K94 and K96 (TD for Turnover-Defective), red; (González and Cullen,
301 2022)]. We next sought to identify lysine residues required for degradation of Cdc42p at 37ºC.
302 Systematic examination of lysine substitutions introduced into GFP-Cdc42p identified one lysine
303 residue in the C-terminal region (K166) and four in the poly-basic C-terminal domain (PB) that
304 were required for the reduced levels of Cdc42p seen at 37ºC (**Fig. 2B,** 37ºC). Other lysine residues
305 were not required (**Fig. 2C**; levels, 37ºC). In particular, the three lysine residues required for the
306 reduction in levels of GTP-Cdc42p did not impact the levels of Cdc42p at 37˚C (**Fig. 2B,** Q61L+
307 TD, K5R, K94R, K96R). In line with this result, K166R and four lysines in the PB region were
308 not required for degradation of a GTP-locked version of Cdc42p (**Fig. 2B,** Q61L), indicating that
309 each context requires non-overlapping lysine residues (**Fig. 2, A** and **C**). Some combinations of
310 lysine substitutions did not promote the stability of the protein (**Fig. 2C**, K166R, K183R, K184R,
311 K186R, K187R; K5, K123, K128, K166R; 12KR; 13KR), which indicates that lysines can play
312 roles in protein turnover (see below). Therefore, we suggest that a subset of lysine residues target
313 the degradation of Cdc42p at 37ºC (polybasic; K166) while others are required for degradation of
314 GTP-locked Cdc42p (TD). Thus, different lysines are needed in different settings.

315

316 ***Cdc42p is turned over at 37˚C by two pathways: by the proteasome and by the vacuole in an***
317 ***ESCRT-dependent manner***

318 Proteins can be degraded by intracellular trafficking in the lysosome called the vacuole in yeast
319 (Perera and Zoncu, 2016) and by the 26S proteasome (Grice and Nathan, 2016). Although Cdc42p
320 is a cytosolic protein (which favors proteasome degradation), it also is modified by a lipid anchor
321 and is associated with membranes (perhaps favoring vacuolar degradation). At 37˚C, GFP-Cdc42p
322 accumulated in the *cim3-1* mutant (also known as *rpt6-1*), which is defective for proteasome
323 function (Ghislain et al., 1993) (**Fig. 3A,** similar data was reported in (González and Cullen, 2022).
324 *PEP4* encodes a vacuolar protease that is required for maturation and activation of vacuolar
325 proteases (Parr et al., 2007). The *pep4*Δ mutant also showed elevated Cdc42p levels at 30ºC and
326 37ºC (**Fig. 3B**; time 0). Time course analysis revealed that GFP-Cdc42p levels at 37ºC were higher
327 in the *pep4*Δ mutant (half-life ≈ 100 min) than seen in wild-type cells (half-life ≈ 22 min) (**Fig.**
328 **3B**), indicating that the vacuole is required for Cdc42p degradation under physiological conditions
329 and upon heat stress (37ºC). Immunoblot analysis also showed that cleavage of GFP from GFP-
330 Cdc42p, which is commonly mediated by vacuolar proteases (Hettema et al., 2004), was dependent
331 on Pep4p (**Fig. 3C**). Taken together, these results indicate that Cdc42p can be turned over by the
332 26S proteasome and also by a mechanism that involves trafficking of ~~the~~ proteins for turnover in
333 the vacuole.

334 We further examined the role of the trafficking pathway on Cdc42p degradation at 37ºC.
335 The ESCRT complex regulates the invagination of proteins from the surface of endosomes to the
336 MVB (Remec Pavlin and Hurley, 2020), which after fusion with the vacuole results in the
337 degradation of cargo proteins (Henne et al., 2011). ESCRT is made up of several protein complexes
338 [ESCRT-0, ESCRT-I, ESCRT-II, ESCRT-III and the Vps4p complex] (Banjade et al., 2021;

Remec Pavlin and Hurley, 2020; Strohacker et al., 2021). We examined the levels of Cdc42p in cells lacking Vps22p, which is a component of the ESCRT-II complex (Hierro et al., 2004). At 37ºC, turnover of GFP-Cdc42p was defective in cells lacking Vps22p during the first 60 min (**Fig. 3D;** half-life in WT cells < 5min; half-life in *vps22*Δ ≈ 40 min), which indicates that ESCRT is required for Cdc42p degradation at initial time points. However, GFP-Cdc42p was degraded at 120 min in cells lacking Vps22p, suggesting that prolongated incubation of cells at 37ºC induces the degradation of Cdc42p in an ESCRT-independent manner. Similar to Vps22p, prolonged incubation at 37ºC induced Cdc42p degradation in the *pep4*Δ mutant (**Fig. 3B**; 120 min). These results indicate that the vacuole contributes to Cdc42p turnover at 37ºC; however, the proteasome makes a more prominent contribution.

Time-lapse fluorescence microscopy also showed accumulation of GFP-Cdc42p in cells lacking Vps22p (**Fig. 3D**). Quantification of the fluorescence signal showed that the reduction in GFP-Cdc42p levels at 37˚C was dependent on Vps22p (**Fig. 3E**). Therefore, the 26S proteasome and the trafficking pathway (an ESCRT-dependent pathway that culminates in the vacuole) regulate the degradation of Cdc42p under physiological and heat stress (37ºC) conditions.

Rsp5p mediates the turnover of plasma membrane proteins through the trafficking pathway to the vacuole (Gajewska et al., 2001; Lauwers et al., 2010). Cdc42p is associated with the plasma membrane by prenylation, which occurs by modification of the cysteine at position C188 (Ziman et al., 1991). We tested whether a version of Cdc42p that cannot be prenylated, GFP-Cdc42p^{C188S}, was capable of being turned over in the trafficking pathway. Cells lacking Vps22p did not influence GFP-Cdc42p^{C188S} localization (**Fig. 4A**), which was mainly cytoplasmic. In addition, ~~and~~ the cleavage of GFP from GFP-Cdc42p^{C188S}, which indicates vacuolar degradation, was significantly reduced (**Fig. 4**, **B** and **C**). These results indicate that Cdc42p localization at the

plasma membrane is critical for its internalization to endosomes and for ESCRT-dependent turnover in the vacuole. Taken together, these data show that a Rho-type GTPase can be turned over in by an ESCRT-dependent vacuolar pathway.

The ESCRT pathway and vacuole are not required for turnover of GTP-locked Cdc42p

When bound to GTP, Cdc42p binds to effector proteins to exert its biological functions. Cdc42p^{Q61L} has some abnormal properties (Woods and Lew, 2019), but it mimics the GTP-locked version of the protein (Ziman et al., 1991), localizes to the plasma membrane (Woods et al 2016), and hyperactivates the mating and fMAPK pathways (Gonzalez and Cullen 2022). In a previous study, we found that GTP-locked Cdc42p is turned over by the 26S proteasome to attenuate the activity of a MAPK pathway that regulates filamentous growth (González and Cullen, 2022). The fact that wild-type Cdc42p was turned over in the trafficking pathway prompted us to investigate whether the turnover of GTP-Cdc42p might also occur in the ESCRT-to-vacuole pathway, which might be important to regulate Cdc42p activity. We compared localization of GFP-Cdc42p to Msb2p-GFP, a transmembrane signaling glycoprotein that is known to be degraded in an ESCRT (Adhikari et al., 2015b). In wild-type cells, Msb2p-GFP was mainly found inside the vacuole due to the high rate of turnover of the protein (**Fig. 5A**, WT, Msb2p-GFP). Msb2p-GFP colocalized with the FM4-64 dye in the MVB in cells lacking Vps22p (**Fig. 5A**, *vps22*Δ, Msb2-GFP) and accumulated in the MVB in cells lacking several ESCRT components (**Fig. 5B**, left, Msb2-GFP). GFP-Cdc42p colocalized with FM4-64 in wild-type cells and was trapped in the MVB in cells lacking Vps22p (**Fig. 5A,** *vps22*Δ, GFP-Cdc42). GFP-Cdc42p also piled up in MVB in several ESCRT components (**Fig. 5B**, middle, GFP-Cdc42), corroborating that ESCRT is required for Cdc42p localization to MVB. However, GFP-Cdc42p^{Q61L}, which tightly localizes to the plasma

membrane [**Fig. 5**A WT, GFP-Cdc42^{Q61L}; (Woods et al., 2016a)], did not show colocalization with FM4-64 in cells lacking Vps22p (**Fig. 5A**, *vps22*Δ, GFP-Cdc42^{Q61L}) or in any ESCRT component examined (**Fig. 5B**, left, GFP-Cdc42^{Q61L}). Consistently, the level of GFP-Cdc42p^{Q61L} was not stabilized in cells lacking Pep4p at either temperature (**Fig. 5C**, compare to **Fig. 3B**). In fact, the *pep4Δ* mutant showed reduced levels of Cdc42p^{Q61L} compared to wild-type cells, which may occur because cells lacking Pep4p may be more efficient at degrading Cdc42p by the proteasome. Moreover, although the degradation of GFP-Cdc42p^{Q61L} was induced at 37ºC (**Fig. 5D**). Its localization was not influenced in cells lacking Vps22 (ESCRT-II) (**Fig. 5E**). These results support previous findings that GFP-Cdc42p^{Q61L} is turned over by the proteosome (González and Cullen, 2022). Taken together, these results suggest that GTP-locked Cdc42p is not turned over by ESCRT in the trafficking pathway at 30ºC or 37ºC.

Turnover of Cdc42 at 37ºC impairs the response to mating pheromone and impacts cell growth

High temperatures might induce Cdc42p mis-folding, resulting in turnover of the inactive version of the protein. Alternatively, Cdc42p turnover at high temperatures might be a regulated response that influences one or more of its functions in the cell. To test this possibility, we first looked at the mating response, which is regulated by a Cdc42p-dependent MAPK pathway (Bardwell, 2005; Chen et al., 2000; Good et al., 2009; Herskowitz, 1995; Kim and Rose, 2022; Li et al., 2017). The addition of α-factor causes cell cycle arrest in the G1 phase of the cell cycle (halo formation) and can be used to measure the activity of the mating pathway (Butty et al., 1998; Long et al., 1997). We found that halo size declined as temperature increased (**Fig. 6**, **A** and **B**), indicating that mating is compromised at high temperatures. This could be a result of Cdc42p turnover at high temperatures. Pheromone sensitivity was restored in cells lacking Ydj1p (**Fig. 6**, **A** and **B**), which

have elevated levels of Cdc42p (**Fig. 1D**). Taken together these results suggest that Cdc42p turnover at high temperature impacts Cdc42p functions in the cell.

We next asked whether Cdc42p stabilization by lysine substitutions impacts the mating response. Lysine substitutions in the poly-basic C-terminus (PB) did not significantly impact halo formation, but K166A (also containing R163A) caused the formation of larger haloes specifically at high temperatures (**Fig. 6, C** and **D**; 34ºC), which corroborates the idea that Cdc42p might be degraded at high temperatures to impact its functions in the cell. GTP-Cdc42p does not impact mating at 30˚C [(González and Cullen, 2022)]. However, a turnover-defective (TD) version of GTP-locked Cdc42p, $Cdc42p^{Q61L+TD}$ ($Cdc42p^{Q61L,K5R,K94R,K96R}$), also formed larger haloes at 37ºC (**Fig. 6, E** and **F**). This result reinforces the idea that turnover of GTP-Cdc42p attenuates mating at 37ºC. It should be noted that the K5R, K94R, and K96R did not impact total Cdc42p levels at 37ºC (**Fig. 2B**), suggesting that these three lysines might be exclusively targeted for degradation of the GTP-bound conformation, either at 30ºC or 37ºC. Cdc42p also regulates the fMAPK and HOG pathways, which were not tested here.

Cdc42p stimulates bud growth through the binding to different effector proteins, which is coordinated with the cell cycle (Miller et al., 2020; Moran et al., 2019). We next explored whether preventing Cdc42p degradation at high temperatures impacts cell viability. $Cdc42p^{PB}$ and $Cdc42p^{R163A,K166R}$ mutants, which prevents Cdc42p degradation at 37ºC, were defective for growth at high temperatures (**Fig. 6G**; 34ºC). Cells defective for Cdc42p turnover at 34ºC were examined by microscopy. Interestingly, cells defective for Cdc42p turnover at 37˚C showed morphological defects compared to wild-type Cdc42p (**Fig. 6H**; PB; R163A, K166A). Cells were elongated and showed hyperpolarized growth. These morphologies were suggestive of defects in septin organization, and consistent with this hypothesis, fluorescence microscopy showed that cells had

multiple septin rings (**Fig. 6H**; Cdc3-mCherry; arrows). The phenotypes observed were different than phenotypes described for accumulation of GTP-Cdc42p (González and Cullen, 2022). Taken together, these results indicate that turnover of Cdc42p at high temperatures has functional consequences in a subset of Cdc42p-dependent processes. Failure to degrade Cdc42p in this setting has detrimental consequences on cell fitness and cell polarity.

Lysine residue K16 is required for stability of Cdc42p

By analyzing the levels of versions of Cdc42p containing lysine substitutions, we found that some versions showed reduced levels compared to wild type (**Fig. 7A**). These included eight versions of the protein tested that contained lysine substitutions in different parts of the protein (**Fig. 6B**). The low levels of Cdc42p presumably result from enhanced turnover. We traced the stability defect of Cdc42p to a single residue, K16, a lysine residue that is located in the P-loop of the protein and which is not surface exposed. Versions of Cdc42p that contained the substitution K16R were found at low levels in the cell (**Fig. 6**, **A**-**C**, shown in green).

Incidentally, the fact that GFP-Cdc42p^{13KR} was stabilized in the in the *cim3-1* proteasome mutant (**Fig. 7D**) was intriguing because Cdc42p^{13KR} does not contain any lysine residues. This version of the protein was also present at low levels in the cell (**Fig. 6B**, 13KR). This data suggests that this version of Cdc42p can be turned over in a manner that does not require lysine residues, which is unexpected because protein ubiquitination typically occurs on lysine residues (Hochstrasser, 2000). To confirm this possibility, the GFP epitope, (which does contain lysine residues), was substituted by a Hisx6 tag. The Hisx6-Cdc42p^{13KR} protein that lacks any lysine residues was also present at low levels (**Fig. 7E)** suggesting that this version of Cdc42p might be

degraded even when lysines are not available. In some proteins, cysteine, serine, and threonine can act as ubiquitin acceptors (Kravtsova-Ivantsiv and Ciechanover, 2012; Lei et al., 2018; McClellan et al., 2019; McDowell and Philpott, 2013; Tait et al., 2007; Wang et al., 2007). Alternatively, Cdc42p aggregates might be degraded by the 26S proteasome in an ubiquitin-independent manner, as has been recently shown for some membranelles condensates (Carrettiero et al., 2022), and for the degradation of the Tau protein, which shows high intracellular accumulation in Alzheimer's disease (Grune et al., 2010; Ukmar-Godec et al., 2020).

Accumulation of Cdc42p^{K16R}, or overexpression of the protein, leads to the formation of aggregates

The localization of unstable versions of GFP-Cdc42p was examined by fluorescence microscopy, which confirmed that these proteins are present at low levels in the cell (**Fig. 7B**). The localization of these proteins was also examined in the *cim3-1* mutant at 37ºC, where these unstable proteins would be expected to accumulate. Compared to wild-type GFP-Cdc42p (**Fig. 7B**; GFP-Cdc42 ≥ 0.5), which showed a normal localization pattern (**Fig. 7, F** and **G**), versions of Cdc42p that were found at reduced levels (**Fig. 7B**; GFP-Cdc42 ≤ 0.2) showed a punctuate pattern indicative of protein aggregates (**Fig. 7G**). For example, Cdc42p^{13KR} accumulated in cells lacking a functional proteasome based on immunoblot analysis (**Fig. 7D**) and formed aggregates in the *cim3-1* mutant (13KR; **Fig. 7F**). Therefore, the turnover of Cdc42p^{13KR} occurs in the 26S proteasome to inhibit the accumulation of protein aggregates.

As for protein stability, the formation of aggregates of GFP-Cdc42p^{13KR} was traced to the lysine residue, K16. Cdc42p^{K12R}, which lacks all of the lysines in Cdc42p except K16, showed a

normal localization pattern (**Fig. 7F**; 12KR). Likewise, GFP-Cdc42p^{K16R}, which contains only a single lysine substitution at position K16, formed aggregates (**Fig. 7F**; K16R). We furthermore saw a direct correspondence between versions of Cdc42p containing K16R, reduced protein levels (< 0.2), and aggregate formation (**Fig. 7C**). Given there are few examples of aggregate formation of Rho-type GTPases, this phenotype was examined in more detail.

We first asked whether wild-type versions of Cdc42p were capable of forming aggregates. Growth at 37˚C did not induce aggregation of GFP-Cdc42p (**Fig. 7F,** no Change), but overexpression of the *GFP-CDC42* gene from a strong inducible promoter (P_{GAL1}) induced a punctate localization pattern in some cells (**Fig. 8A**, ~20% of cells, t = 6h). Therefore, the wild-type Cdc42p protein is capable of forming aggregates when overproduced.

For many proteins, aggregates are retained in mother cells, which occurs by a Ydj1p-(HSP40-) dependent mechanism (Saarikangas et al., 2017), presumably to ensure that properly folded proteins are enriched in daughter cells to promote cellular rejuvenation (Hill et al., 2017). When overexpressed, Cdc42p aggregates preferentially accumulated in mother cells (**Fig. 8A**). The filamentous strain background (Σ1278b) was used to facilitate the assessment of cell lineage, because adhesive cells fail to separate. GFP-Cdc42p^{K16R} aggregates were also enriched in mother cells in the *cim3-1* mutant (**Fig. 8B**; Movie 1, control GFP-Cdc42p; Movie 2, GFP-Cdc42p^{K16R}).

We next explored the localization of GFP-Cdc42p in mother cells using the Mother Enrichment Program (MEP) (Lindstrom and Gottschling, 2009; Moreno et al., 2019). We observed some GFP-Cdc42p aggregates in older cells, however, unexpectedly, GFP-Cdc42p also formed aggregates in young cells (**Fig. 8C,** arrows). Therefore, we could not establish a correlation between age and Cdc42p aggregates using this approach. Young cells in the MEP program lack

497 the anaphase-promoting complex (APC) activator *CDC20*, which fails to degrade mitotic cyclins
498 required for cell cycle progression (Visintin et al., 1997). Thus, aggregated Cdc42p in those cells
499 might occur due to defective protein degradation of Cdc42p or perhaps due to general proteostatic
500 stress. Analysis of GFP-Cdc42p in older cells, also revealed low levels of GFP-Cdc42p at the
501 plasma membrane compared to arrested daughter cells (**Fig. 8D**), which might be expected as these
502 cells lose their ability to form buds. Although the formation of aggregates might in principle cause
503 deleterious phenotypes, overexpression of GFP-Cdc42p or aggregates induced by K16R did not
504 cause a noticeable growth defect (shown for **Fig. 8B;** Movie 2). Therefore, Cdc42p can form
505 aggregates when overproduced or when versions of the protein that compromise stability
506 accumulate to high levels in the cell.

507

508 **DISCUSSION**

509 Rho GTPases govern many aspects of cellular function including cytoskeletal dynamics and signal
510 transduction pathways to control a wide range of biological responses. Altered Rho GTPase
511 regulation impacts human health, including for example the induction of malignant transformation
512 in some cancers (Goka and Lippman, 2015; Huang et al., 2013; Tamehiro et al., 2015; Zhang et
513 al., 2019) and is an underlying cause of some neurological (Aguilar et al., 2017; Guiler et al., 2021)
514 and immunological diseases (El Masri and Delon, 2021). Understanding the regulatory
515 determinants of Rho GTPase stability can provide insights into how these proteins are regulated
516 and may impact our understanding of the roles these regulatory features play in the healthy and
517 disease states. We found that Cdc42p is degraded by two routes. One route required the ESCRT-
518 to-vacuole pathway, and the other required the 26S proteasome and occurred in an HSP-dependent
519 manner. A specific environmental condition, 37ºC, triggered degradation of the protein and

negatively impacted a Cdc42p-dependent MAPK pathway that controls the ability of haploid cells to mate. Interestingly, Cdc42p turnover at 37ºC promoted cell viability and reduced polarity defects, which might indicate that Cdc42p degradation represents one way for an organism to control the tradeoff between viability and reproduction, which might be conserved in higher eukaryotes. We identified residues that were required for turnover at 37˚C as well as one residue that promotes the formation of Cdc42p aggregates in certain genetic contexts. Therefore, by exploring the turnover regulation of the Rho GTPase Cdc42p in yeast, new and potentially general insights into aspects of Rho GTPase regulation were uncovered that may extend to other systems.

Rho GTPase turnover at high temperatures: identification of lysines and elucidation of the turnover mechanism

We previously showed that chaperones of the HSP40 and HSP70 family and the NEDD4-type ubiquitin ligase Rsp5p were required for turnover of GTP-Cdc42p, and we identified lysines involved in its turnover [TD: K5, K94, and K96 (González and Cullen, 2022)]. Here, we show that Cdc42p is degraded in response to growth at high temperatures, which requires the same HSP40, HSP70, and Rsp5p proteins and a different set of lysine residues (K166; PB **Fig. 7**). Lysines that impact turnover of a GTP-locked version of Cdc42p (Q61L also containing TD: K5, K94, and K96) are distinct from lysines that promote turnover of the protein at 37˚C (PB and K166). Evidence for this conclusion comes from the fact that introduction of the lysine substitutions in a version of Cdc42p also harboring Q61L show different protein levels than substitutions that affect protein levels at 37˚C (**Fig. 2**), and from the fact that pheromone, which actives Cdc42p (Simon et al., 1995), does not show different sized haloes in versions of the protein carrying PB and K166R under normal growth conditions. The fact that GTP-Cdc42p requires different lysine residues than degradation of the protein at 37ºC might be

543 important, since GTP-Cdc42p degradation only impacts the active state of the protein (presumably
544 a small fraction of the protein), while at 37ºC most of the protein in the cell is degraded. Different
545 lysines may target the protein for turnover perhaps because the conformation of Cdc42p might
546 change in different ways in response to GTP binding and protein folding at high temperatures,
547 which may impact lysine accessibility by Rsp5p, or recognition of different parts of the protein by
548 HSPs. Alternatively, the exposure of lysines might be influenced by different Cdc42p-interacting
549 proteins that bind Cdc42p in the two contexts. Cdc42p turnover at 37ºC was mediated by the 26S
550 proteasome and the vacuole. Given that that proteasomes become more active upon heat shock in
551 mammalian cells (Lee and Goldberg, 2022), this temperature-dependent activation of proteasome
552 function might favor the degradation of Cdc42p by the proteasome under this condition.

553 Cdc42p is a highly conserved protein from yeast to humans. We have identified conserved
554 lysines in the Cdc42p protein that are important for turnover of the protein at 37˚C. Cdc42p^{K166R}
555 is resistant to degradation at high temperatures. Based on cBioPortal for Cancer Genomics, K166
556 is a hotspot for cancer mutation in CDC42 (Crosas-Molist et al., 2022). It would be interesting to
557 explore whether mutations at that site lead to elevated protein levels in malignant cells. We also
558 identified residues in the polybasic domain that contribute to turnover. In humans, CDC42 has two
559 splice variants (Hart et al., 1991; Olenik et al., 1999)
560 that differ in nine amino acids at the C-terminus of the protein. CDC42 plays an essential role
561 during early mammalian development (Chen et al., 2000), and recently it has been shown that the
562 two isoforms perform antagonist functions during neural differentiation, in particular by
563 controlling mTOR activity (Endo et al., 2020). It is not clear how almost identical proteins are
564 specificality regulated to perform different functions in the cell. The lysines K183 and K184,
565 which we found were required for degradation of Cdc42p at 37ºC, are present in one splice variant

but not another. K183 and K184 may target one variant of CDC42 for degradation, allowing the other variant to perform its functions in neural development. Generally speaking, mutations that lead to the upregulation of Rho GTPases might contribute to malignant transformation and cancer metastasis (Clayton and Ridley, 2020; Hodge et al., 2020) and potentially problems in development.

The biological relevance of Rho GTPase turnover at high temperatures

Heat shock stress induces protein misfolding, and cells respond by promoting protein refolding and clearing damaged proteins by degradation in an HSP-dependent manner, since accumulation of misfolded protein can cause damage to cell function and viability (Klaips et al., 2018; Sala et al., 2017). Cdc42p may be turned over at high temperatures as a type of protein quality control mechanism to prevent protein misfolding. However, evidence here suggests that the turnover of Cdc42p at elevated temperatures also has functional relevance to biological processes. We specifically found that cells respond poorly to pheromone at elevated temperatures. Thus, cells may experience a tradeoff, favoring protein folding/stability at the expense of mating, which itself is a key driver of evolutionary fecundity. Turnover of active Cdc42p did not impact mating at 30ºC, maybe because there are enough levels of the protein to reach the maximum activity required. However, at 37ºC when the levels of Cdc42p are reduced, mating sensitivity also becomes reduced. Maybe this is a priority for Cdc42p functions, which depend on the available levels of Cdc42p. Interestingly, incubation at 37ºC (body temperate) decreases a switch in cell type (from white to opaque cells) of the human pathogen *Candida albicans* that is required for mating

(Johnson, 2003), indicating that mating deficient at 37ºC might be a feature conserved across species.

Cdc42p turnover at 37ºC might occur by recognition of the misfolded protein by HSP protein chaperones. However, preventing the degradation of Cdc42p at 37ºC by deletion of Ydj1p or stabilization of Cdc42p by K166 mutation induced better activation of the mating pathway, which is regulated by Cdc42p. This indicates that at least some fraction of Cdc42p may be turned over to shut down the function of the protein. Preventing Cdc42p degradation at high temperatures negatively influenced cell viability. This suggests that degradation of Cdc42p at 37ºC might be a coordinated response to inhibit any Cdc42p functions. At 37ºC, the PKC pathway gets activated to repair cell wall damage in yeast (Levin, 2011). The Rho GTPase Rho1p, which shares downstream effectors with Cdc42p, regulates the PKC pathway to control aspects of polarized growth and morphogenesis (Andrews and Stark, 2000; Bettinger et al., 2007; Delley and Hall, 1999; Kono et al., 2012). During cytokinesis, Rho1p and Cdc42p function antagonistically, while Rho1p promotes actomyosin ring assembly and secondary septum formation, Cdc42p inhibits the formation of the secondary septum (Atkins et al., 2013; Onishi et al., 2013; Tolliday et al., 2002; Yoshida et al., 2009). This inhibitory effect of Cdc42p during cytokinesis was mediated by the GAP Bem2p and the PAK kinase Ste20p (Atkins et al., 2013). We found here that preventing Cdc42p degradation impacted cell separation at high temperatures, where cells showed multiple septin rings within the same cell. These observations suggest that Cdc42p turnover regulation under this condition may be required for proper cytokinesis. In this way, Cdc42p turnover regulation may impact Rho1p-dependent responses, to ensure cell wall repair through the PKC pathway and effective cell separation.

609 Intriguingly, the turnover of Cdc42p at 37˚C may represent an example at the molecular
610 level of the tradeoff between mating and cellular fitness. An ongoing goal of evolutionary biology
611 is to identify the causes of sexual selection and diversification, including sexual selection,
612 phenotypic diversity, and tradeoffs between mating and fitness in other contexts. Here, we
613 unexpectedly found that cells sensitivity to mating pheromone is reduced at higher temperatures,
614 suggesting that mating under this condition is not preferred. We show that was at least in part due
615 to Cdc42p turnover under this condition. We further show that by restoring Cdc42p levels, we
616 could restore pheromone sensitivities at higher temperatures, but this came at a cost to cell growth
617 (or viability), corresponding to polarity defects. Therefore, Cdc42p activity promoting mating
618 under one condition can lead to a trade off in overall fitness. This provides one of many such
619 examples of tradeoffs to be identified (Johnston et al., 2013), here in this case shown by altering
620 the levels of a regulatory GTPase in a condition-specific manner.

621

622 ***Rho GTPase turnover occurs in an ESCRT-dependent manner in the vacuole***

623 Transmembrane proteins at the plasma membrane can be ubiquitinated for targeting by turnover
624 in the secretory pathway. By comparison, cytosolic proteins are typically turned over by the
625 proteasome. Rho GTPases represent a special case, because they are cytosolic proteins that
626 associate with the plasma membrane by the addition of a lipid anchor. This feature may account
627 for why Cdc42p is turned over by both the proteasome and in the trafficking pathways. Indeed, we
628 found that versions of Cdc42p that cannot be lipid modified are not turned over by ESCRT. In
629 both cases, the turnover of Cdc42p requires Rsp5p, which can function to control protein turnover

630 in the cytoplasm, yet is also responsible for most if not all turnover of proteins at the plasma
631 membrane.

632 Although this may be the first case for turnover of a Rho GTPase in the trafficking pathway,
633 other types of GTPases follow a similar route. For example, RAS can also be degraded in a
634 lysosome- (Lu et al., 2009) and proteasome-dependent manner (Jeong et al., 2018; Kim et al.,
635 2009), which both lead to attenuation in MAPK signaling. The alpha subunit of heterotrimeric G-
636 proteins, such as the mating pathway Gα subunit Gpa1p, also undergoes proteasomal and vacuolar
637 degradation (Dohlman and Campbell, 2019). This differential regulation of Cdc42p might allow
638 specificity in the degradation of Cdc42p in response to different stimuli. For example, GTP-
639 Cdc42p is turned over mainly in by the proteasome, whereas at 37˚C, Cdc42p is turned over by
640 both the proteasome and the vacuole. Alternative routes for Cdc42p degradation might be
641 beneficial for accelerating Cdc42p turnover in specific contexts and in response to different
642 stimuli. It will be interesting to determine whether the trafficking pathway is required for
643 degradation of other Rho GTPases or CDC42 in humans and other systems.

644

645 ***Determinants of Rho GTPase stability and the formation of protein aggregates in aging cells***

646 Protein aggregates are assemblies formed by association of misfolded proteins mainly connected
647 through hydrophobic interactions that accumulate in the intracellular environment (Balchin et al.,
648 2016). Many cytosolic proteins and mRNAs can form aggregates, which can occur in a highly
649 regulated manner in response to nutrient limitation and other stresses and which can also lead to
650 cellular stress and aging (Alshareedah et al., 2020; Cabrera et al., 2020; Hill et al., 2017; Khong
651 and Parker, 2020; Moreno et al., 2019; Samant et al., 2018). In mammals, accumulation of protein

aggregates is a major cause of folding-related neurodegenerative disorders (Balchin et al., 2016; Dobson, 2002). We found that a single lysine residue in the Cdc42p protein that is not surface exposed (K16) was important for the stability of the protein. K16 has previously been shown to be required for Cdc42p function, as that mutation expressed endogenously is inviable (Kozminski et al., 2000). Thus, the instability of Cdc42p^{K16R} might account for its inability to function in the cell. When expressed in cells that fail to turn over Cdc42p (e.g. proteasome mutant), Cdc42^{K16R} forms protein aggregates. Despite the fact that many proteins have been shown to form cytosolic aggregates, few examples have been reported for Rho GTPases. Interestingly, high temperatures induce aggregation of another Rho GTPase, Rho1p^{C17R}-GFP in fission yeast. In this case, the GFP tag inhibits the prenylation of Rho1p, and the protein forms aggregates when not targeted to the plasma membrane (Cabrera et al., 2020). Therefore, the stability of Rho GTPases, as well as their membrane localization, may contribute to the aggregation of the protein. We also found that overproduction of wild-type versions of Cdc42p can form aggregates. The formation of aggregates might be a mechanism to maintain Cdc42p protein levels within the stoichiometric limits forced by physical or functional protein interactions. Interestingly, Cdc42p aggregates – due to overexpression or misfolding (K16R) - were partitioned to mother cells, presumably as part of the protein rejuvenation response (Hill et al., 2017). Therefore, as is true for many protein quality control drivers (Santra et al., 2019), Rho aggregation may impact aging in cells. Furthermore, the same point mutation that causes Cdc42p aggregates, K16R, was found in patients with pancreatic cancer (cBioPortal for Cancer Genomics), which might suggest that alterations in that part of the protein are critical for its folding and stability.

ABBREVIATIONS

675 CHX, cycloheximide; DIC, differential interference contrast; Glu, glucose; Gal, galactose; GAP,
676 GTPase activating protein; GEF, guanine nucleotide exchange factor; GFP, green fluorescent
677 protein; GTPase, guanine nucleotide triphosphate; HMW, high molecular weight; HR,
678 homologous recombination; HSP, heat shock protein; kDa, kilodalton; MAPK, mitogen-activated
679 protein kinase; MVB, multivesicular bodies; fMAPK, filamentous growth MAP kinase pathway;
680 O.D., PAK, p21-activated kinase; PB, polybasic; Rho, Ras homology; S. D., standard deviation;
681 SDM, site-directed mutagenesis; SDS-PAGE, sodium dodecyl sulfate-polyacrylamide gel
682 electrophoresis; YEPD, yeast extract, peptone and dextrose; WT, wild type.
683

684 **ACKNOWLEDGEMENTS**

685 Thanks to Charles Boone (University of Toronto), Keith Kozminski (University of Virginia,
686 Charlottesville, VA), Daniel Lew (Duke University, Raleigh NC), David Pellman (Harvard
687 Medical School, Boston, MA), and Scott Emr (Cornell University, Ithaca, NY) for providing
688 reagents. Thanks to Emily Mehle for assistance with experiments and lab members for suggestions.
689 Thanks to Atindra Pujari for the construction of the pRS313-CDC3-mCherry::HYG plasmid. The
690 work was supported by a grant from the NIH (GM098629).
691

692 ***Data Availability Statement***

693 Strains, plasmids, and other reagents generated for the study are freely available upon request (to
694 P.J.C.). All of the data for the manuscript is included in the main body and is also available here
695 (https://pjcullen.wixsite.com/labsite/mcb-data).
696

697 ***Declaration of Interest Statement***

698 The authors declare no conflict of interests in the design or execution of the study.

699

700 **REFERENCES**
701

702 Adamo, J.E., J.J. Moskow, A.S. Gladfelter, D. Viterbo, D.J. Lew, and P.J. Brennwald. 2001.
703 Yeast Cdc42 functions at a late step in exocytosis, specifically during polarized growth of
704 the emerging bud. *J Cell Biol*. 155:581-592.
705 Adhikari, H., L.M. Caccamise, T. Pande, and P.J. Cullen. 2015a. Comparative Analysis of
706 Transmembrane Regulators of the Filamentous Growth Mitogen-Activated Protein
707 Kinase Pathway Uncovers Functional and Regulatory Differences. *Eukaryotic Cell*.
708 14:868-883.
709 Adhikari, H., N. Vadaie, J. Chow, L.M. Caccamise, C.A. Chavel, B. Li, A. Bowitch, C.J. Stefan,
710 and P.J. Cullen. 2015b. Role of the unfolded protein response in regulating the mucin-
711 dependent filamentous-growth mitogen-activated protein kinase pathway. *Mol Cell Biol*.
712 35:1414-1432.
713 Aguilar, B.J., Y. Zhu, and Q. Lu. 2017. Rho GTPases as therapeutic targets in Alzheimer's
714 disease. *Alzheimer's Research & Therapy*. 9:97.
715 Aguilar, R.C., S.A. Longhi, J.D. Shaw, L.Y. Yeh, S. Kim, A. Schön, E. Freire, A. Hsu, W.K.
716 McCormick, H.A. Watson, and B. Wendland. 2006. Epsin N-terminal homology domains
717 perform an essential function regulating Cdc42 through binding Cdc42 GTPase-
718 activating proteins. *Proc Natl Acad Sci U S A*. 103:4116-4121.
719 Albakova, Z., Y. Mangasarova, A. Albakov, and L. Gorenkova. 2022. HSP70 and HSP90 in
720 Cancer: Cytosolic, Endoplasmic Reticulum and Mitochondrial Chaperones of
721 Tumorigenesis. *Front Oncol*. 12:829520.
722 Alshareedah, I., M.M. Moosa, M. Raju, D.A. Potoyan, and P.R. Banerjee. 2020. Phase transition
723 of RNA−protein complexes into ordered hollow condensates. *Proceedings of the*
724 *National Academy of Sciences*. 117:15650-15658.
725 Amberg, D.C., D.J. Burke, and J.N. Strathern. 2006. Yeast Vital Stains: Visualizing Vacuoles
726 and Endocytic Compartments with FM4-64. *CSH Protoc*. 2006.
727 Amm, I., T. Sommer, and D.H. Wolf. 2014. Protein quality control and elimination of protein
728 waste: the role of the ubiquitin-proteasome system. *Biochim Biophys Acta*. 1843:182-196.
729 Andrews, P.D., and M.J. Stark. 2000. Dynamic, Rho1p-dependent localization of Pkc1p to sites
730 of polarized growth. *J Cell Sci*. 113 (Pt 15):2685-2693.
731 Arrazola Sastre, A., M. Luque Montoro, P. Gálvez-Martín, H.M. Lacerda, A.M. Lucia, F.
732 Llavero, and J.L. Zugaza. 2020. Small GTPases of the Ras and Rho Families Switch
733 on/off Signaling Pathways in Neurodegenerative Diseases. *Int J Mol Sci*. 21.
734 Atkins, B.D., S. Yoshida, K. Saito, C.-F. Wu, D.J. Lew, and D. Pellman. 2013. Inhibition of
735 Cdc42 during mitotic exit is required for cytokinesis. *J Cell Biol*. 202:231-240.
736 Balchin, D., M. Hayer-Hartl, and F.U. Hartl. 2016. In vivo aspects of protein folding and quality
737 control. *Science*. 353:aac4354.
738 Banjade, S., Y.H. Shah, S. Tang, and S.D. Emr. 2021. Design principles of the ESCRT-III
739 Vps24-Vps2 module. *eLife*. 10:e67709.
740 Bardwell, L. 2005. A walk-through of the yeast mating pheromone response pathway. *Peptides*.
741 26:339-350.
742 Basu, S., B. González, B. Li, G. Kimble, K.G. Kozminski, and P.J. Cullen. 2020. Functions for
743 Cdc42p BEM adaptors in regulating a differentiation-type MAP kinase pathway. *Mol*
744 *Biol Cell*. 31:491-510.

745 Bettinger, B.T., M.G. Clark, and D.C. Amberg. 2007. Requirement for the polarisome and
746 formin function in Ssk2p-mediated actin recovery from osmotic stress in Saccharomyces
747 cerevisiae. *Genetics*. 175:1637-1648.
748 Bi, E., and H.-O. Park. 2012. Cell Polarization and Cytokinesis in Budding Yeast. *Genetics*.
749 191:347.
750 Bos, J.L., H. Rehmann, and A. Wittinghofer. 2007. GEFs and GAPs: critical elements in the
751 control of small G proteins. *Cell*. 129:865-877.
752 Brown, J.L., M. Jaquenoud, M.P. Gulli, J. Chant, and M. Peter. 1997. Novel Cdc42-binding
753 proteins Gic1 and Gic2 control cell polarity in yeast. *Genes & development*. 11:2972-
754 2982.
755 Brückner, S., S. Kern, R. Birke, I. Saugar, H.D. Ulrich, and H.-U. Mösch. 2011. The TEA
756 transcription factor Tec1 links TOR and MAPK pathways to coordinate yeast
757 development. *Genetics*. 189:479-494.
758 Butty, A.C., P.M. Pryciak, L.S. Huang, I. Herskowitz, and M. Peter. 1998. The role of Far1p in
759 linking the heterotrimeric G protein to polarity establishment proteins during yeast
760 mating. *Science*. 282:1511-1516.
761 Cabrera, M., S. Boronat, L. Marte, M. Vega, P. Pérez, J. Ayté, and E. Hidalgo. 2020. Chaperone-
762 Facilitated Aggregation of Thermo-Sensitive Proteins Shields Them from Degradation
763 during Heat Stress. *Cell Reports*. 30:2430-2443.e2434.
764 Carrettiero, D.C., M.C. Almeida, A.P. Longhini, J.N. Rauch, D. Han, X. Zhang, S. Najafi, J.E.
765 Gestwicki, and K.S. Kosik. 2022. Stress routes clients to the proteasome via a BAG2
766 ubiquitin-independent degradation condensate. *Nature Communications*. 13:3074.
767 Chavel, C.A., L.M. Caccamise, B. Li, and P.J. Cullen. 2014. Global regulation of a
768 differentiation MAPK pathway in yeast. *Genetics*. 198:1309-1328.
769 Chen, F., L. Ma, M.C. Parrini, X. Mao, M. Lopez, C. Wu, P.W. Marks, L. Davidson, D.J.
770 Kwiatkowski, T. Kirchhausen, S.H. Orkin, F.S. Rosen, B.J. Mayer, M.W. Kirschner, and
771 F.W. Alt. 2000. Cdc42 is required for PIP(2)-induced actin polymerization and early
772 development but not for cell viability. *Current biology : CB*. 10:758-765.
773 Clayton, N.S., and A.J. Ridley. 2020. Targeting Rho GTPase Signaling Networks in Cancer.
774 *Frontiers in Cell and Developmental Biology*. 8.
775 Coleman, M.L., C.J. Marshall, and M.F. Olson. 2004. RAS and RHO GTPases in G1-phase cell-
776 cycle regulation. *Nat Rev Mol Cell Biol*. 5:355-366.
777 Craig, E.A., and J. Marszalek. 2017. How Do J-Proteins Get Hsp70 to Do So Many Different
778 Things? *Trends Biochem Sci*. 42:355-368.
779 Crosas-Molist, E., R. Samain, L. Kohlhammer, J.L. Orgaz, S.L. George, O. Maiques, J. Barcelo,
780 and V. Sanz-Moreno. 2022. Rho GTPase signaling in cancer progression and
781 dissemination. *Physiological Reviews*. 102:455-510.
782 Cullen, P.J., W. Sabbagh, Jr., E. Graham, M.M. Irick, E.K. van Olden, C. Neal, J. Delrow, L.
783 Bardwell, and G.F. Sprague, Jr. 2004. A signaling mucin at the head of the Cdc42- and
784 MAPK-dependent filamentous growth pathway in yeast. *Genes Dev*. 18:1695-1708.
785 Cullen, P.J., and G.F. Sprague, Jr. 2012. The regulation of filamentous growth in yeast. *Genetics*.
786 190:23-49.
787 Cvrcková, F., C. De Virgilio, E. Manser, J.R. Pringle, and K. Nasmyth. 1995. Ste20-like protein
788 kinases are required for normal localization of cell growth and for cytokinesis in budding
789 yeast. *Genes & Development*. 9:1817-1830.

Delley, P.A., and M.N. Hall. 1999. Cell wall stress depolarizes cell growth via hyperactivation of RHO1. *J Cell Biol*. 147:163-174.
Dobson, C.M. 2002. Getting out of shape. *Nature*. 418:729-730.
Dohlman, H.G., and S.L. Campbell. 2019. Regulation of large and small G proteins by ubiquitination. *The Journal of biological chemistry*. 294:18613-18623.
El Masri, R., and J. Delon. 2021. RHO GTPases: from new partners to complex immune syndromes. *Nature Reviews Immunology*. 21:499-513.
Endo, M., J.E. Druso, and R.A. Cerione. 2020. The two splice variant forms of Cdc42 exert distinct and essential functions in neurogenesis. *The Journal of biological chemistry*. 295:4498-4512.
Etienne-Manneville, S., and A. Hall. 2002. Rho GTPases in cell biology. *Nature*. 420:629-635.
Evangelista, M., K. Blundell, M.S. Longtine, C.J. Chow, N. Adames, J.R. Pringle, M. Peter, and C. Boone. 1997. Bni1p, a yeast formin linking cdc42p and the actin cytoskeleton during polarized morphogenesis. *Science*. 276:118-122.
Evangelista, M., D. Pruyne, D.C. Amberg, C. Boone, and A. Bretscher. 2002. Formins direct Arp2/3-independent actin filament assembly to polarize cell growth in yeast. *Nat Cell Biol*. 4:32-41.
Fang, N.N., G.T. Chan, M. Zhu, S.A. Comyn, A. Persaud, R.J. Deshaies, D. Rotin, J. Gsponer, and T. Mayor. 2014. Rsp5/Nedd4 is the main ubiquitin ligase that targets cytosolic misfolded proteins following heat stress. *Nat Cell Biol*. 16:1227-1237.
Farhan, Y.A.A., M. Arabdin, and A. Khan. 2021. The Role of Heat Shock Proteins in Cellular Homeostasis and Cell Survival. *Cureus*. 13:e18316.
Finley, D., H.D. Ulrich, T. Sommer, and P. Kaiser. 2012. The ubiquitin-proteasome system of Saccharomyces cerevisiae. *Genetics*. 192:319-360.
Florian, M.C., K. Dörr, A. Niebel, D. Daria, H. Schrezenmeier, M. Rojewski, M.D. Filippi, A. Hasenberg, M. Gunzer, K. Scharffetter-Kochanek, Y. Zheng, and H. Geiger. 2012. Cdc42 activity regulates hematopoietic stem cell aging and rejuvenation. *Cell Stem Cell*. 10:520-530.
Gajewska, B., J. Kaminska, A. Jesionowska, N.C. Martin, A.K. Hopper, and T. Zoladek. 2001. WW domains of Rsp5p define different functions: determination of roles in fluid phase and uracil permease endocytosis in Saccharomyces cerevisiae. *Genetics*. 157:91-101.
Geiger, H., and Y. Zheng. 2013. Cdc42 and aging of hematopoietic stem cells. *Curr Opin Hematol*. 20:295-300.
Ghislain, M., A. Udvardy, and C. Mann. 1993. S. cerevisiae 26S protease mutants arrest cell division in G2/metaphase. *Nature*. 366:358-362.
Goka, E.T., and M.E. Lippman. 2015. Loss of the E3 ubiquitin ligase HACE1 results in enhanced Rac1 signaling contributing to breast cancer progression. *Oncogene*. 34:5395-5405.
Goldstein, A.L., and J.H. McCusker. 1999. Three new dominant drug resistance cassettes for gene disruption in Saccharomyces cerevisiae. *Yeast*. 15:1541-1553.
González, B., and P.J. Cullen. 2022. Regulation of Cdc42 protein turnover modulates the filamentous growth MAPK pathway. *Journal of Cell Biology*. 221.
Good, M., G. Tang, J. Singleton, A. Reményi, and W.A. Lim. 2009. The Ste5 scaffold directs mating signaling by catalytically unlocking the Fus3 MAP kinase for activation. *Cell*. 136:1085-1097.

Gorenberg, E.L., and S.S. Chandra. 2017. The Role of Co-chaperones in Synaptic Proteostasis and Neurodegenerative Disease. *Front Neurosci*. 11:248.

Grice, G.L., and J.A. Nathan. 2016. The recognition of ubiquitinated proteins by the proteasome. *Cell Mol Life Sci*. 73:3497-3506.

Grune, T., D. Botzen, M. Engels, P. Voss, B. Kaiser, T. Jung, S. Grimm, G. Ermak, and K.J. Davies. 2010. Tau protein degradation is catalyzed by the ATP/ubiquitin-independent 20S proteasome under normal cell conditions. *Arch Biochem Biophys*. 500:181-188.

Guiler, W., A. Koehler, C. Boykin, and Q. Lu. 2021. Pharmacological Modulators of Small GTPases of Rho Family in Neurodegenerative Diseases. *Front Cell Neurosci*. 15:661612.

Gulli, M.P., M. Jaquenoud, Y. Shimada, G. Niederhäuser, P. Wiget, and M. Peter. 2000. Phosphorylation of the Cdc42 exchange factor Cdc24 by the PAK-like kinase Cla4 may regulate polarized growth in yeast. *Mol Cell*. 6:1155-1167.

Guo, D.F., and K. Rahmouni. 2019. The Bardet-Biedl syndrome protein complex regulates cell migration and tissue repair through a Cullin-3/RhoA pathway. *Am J Physiol Cell Physiol*. 317:C457-c465.

Haga, R.B., and A.J. Ridley. 2016. Rho GTPases: Regulation and roles in cancer cell biology. *Small GTPases*. 7:207-221.

Hart, M.J., K. Shinjo, A. Hall, T. Evans, and R.A. Cerione. 1991. Identification of the human platelet GTPase activating protein for the CDC42Hs protein. *The Journal of biological chemistry*. 266:20840-20848.

Henne, W.M., N.J. Buchkovich, and S.D. Emr. 2011. The ESCRT pathway. *Dev Cell*. 21:77-91.

Herskowitz, I. 1995. MAP kinase pathways in yeast: for mating and more. *Cell*. 80:187-197.

Hettema, E.H., J. Valdez-Taubas, and H.R. Pelham. 2004. Bsd2 binds the ubiquitin ligase Rsp5 and mediates the ubiquitination of transmembrane proteins. *EMBO J*. 23:1279-1288.

Hierro, A., J. Sun, A.S. Rusnak, J. Kim, G. Prag, S.D. Emr, and J.H. Hurley. 2004. Structure of the ESCRT-II endosomal trafficking complex. *Nature*. 431:221-225.

Hill, S.M., S. Hanzén, and T. Nyström. 2017. Restricted access: spatial sequestration of damaged proteins during stress and aging. *EMBO reports*. 18:377-391.

Hochstrasser, M. 2000. Evolution and function of ubiquitin-like protein-conjugation systems. *Nat Cell Biol*. 2:E153-E157.

Hodge, R.G., A. Schaefer, S.V. Howard, and C.J. Der. 2020. RAS and RHO family GTPase mutations in cancer: twin sons of different mothers? *Crit Rev Biochem Mol Biol*. 55:386-407.

Horianopoulos, L.C., and J.W. Kronstad. 2021. Chaperone Networks in Fungal Pathogens of Humans. *Journal of Fungi*. 7.

Huang, T.Y., S. Michael, T. Xu, A. Sarkeshik, J.J. Moresco, J.R. Yates, 3rd, E. Masliah, G.M. Bokoch, and C. DerMardirossian. 2013. A novel Rac1 GAP splice variant relays poly-Ub accumulation signals to mediate Rac1 inactivation. *Mol Biol Cell*. 24:194-209.

Irazoqui, J.E., A.S. Gladfelter, and D.J. Lew. 2003. Scaffold-mediated symmetry breaking by Cdc42p. *Nat Cell Biol*. 5:1062-1070.

Jeong, W.J., E.J. Ro, and K.Y. Choi. 2018. Interaction between Wnt/β-catenin and RAS-ERK pathways and an anti-cancer strategy via degradations of β-catenin and RAS by targeting the Wnt/β-catenin pathway. *NPJ Precis Oncol*. 2:5.

Johnson, A. 2003. The biology of mating in Candida albicans. *Nat Rev Microbiol*. 1:106-116.

Johnston, S.E., J. Gratten, C. Berenos, J.G. Pilkington, T.H. Clutton-Brock, J.M. Pemberton, and J. Slate. 2013. Life history trade-offs at a single locus maintain sexually selected genetic variation. *Nature*. 502:93-95.

Jones, L., K. Tedrick, A. Baier, M.R. Logan, and G. Eitzen. 2010. Cdc42p is activated during vacuole membrane fusion in a sterol-dependent subreaction of priming. *The Journal of biological chemistry*. 285:4298-4306.

Katzmann, D.J., M. Babst, and S.D. Emr. 2001. Ubiquitin-Dependent Sorting into the Multivesicular Body Pathway Requires the Function of a Conserved Endosomal Protein Sorting Complex, ESCRT-I. *Cell*. 106:145-155.

Kawasaki, R., K. Fujimura-Kamada, H. Toi, H. Kato, and K. Tanaka. 2003. The upstream regulator, Rsr1p, and downstream effectors, Gic1p and Gic2p, of the Cdc42p small GTPase coordinately regulate initiation of budding in Saccharomyces cerevisiae. *Genes Cells*. 8:235-250.

Khong, A., and R. Parker. 2020. The landscape of eukaryotic mRNPs. *Rna*. 26:229-239.

Kim, J., and M.D. Rose. 2022. Cla4p Kinase Activity Is Down-Regulated by Fus3p during Yeast Mating. *Biomolecules*. 12.

Kim, S.E., J.Y. Yoon, W.J. Jeong, S.H. Jeon, Y. Park, J.B. Yoon, Y.N. Park, H. Kim, and K.Y. Choi. 2009. H-Ras is degraded by Wnt/beta-catenin signaling via beta-TrCP-mediated polyubiquitylation. *J Cell Sci*. 122:842-848.

Klaips, C.L., G.G. Jayaraj, and F.U. Hartl. 2018. Pathways of cellular proteostasis in aging and disease. *J Cell Biol*. 217:51-63.

Kono, K., Y. Saeki, S. Yoshida, K. Tanaka, and D. Pellman. 2012. Proteasomal degradation resolves competition between cell polarization and cellular wound healing. *Cell*. 150:151-164.

Kozminski, K.G., A.J. Chen, A.A. Rodal, and D.G. Drubin. 2000. Functions and functional domains of the GTPase Cdc42p. *Molecular biology of the cell*. 11:339-354.

Kravtsova-Ivantsiv, Y., and A. Ciechanover. 2012. Non-canonical ubiquitin-based signals for proteasomal degradation. *Journal of Cell Science*. 125:539.

Lamas, I., L. Merlini, A. Vještica, V. Vincenzetti, and S.G. Martin. 2020. Optogenetics reveals Cdc42 local activation by scaffold-mediated positive feedback and Ras GTPase. *PLOS Biology*. 18:e3000600.

Lauwers, E., Z. Erpapazoglou, R. Haguenauer-Tsapis, and B. André. 2010. The ubiquitin code of yeast permease trafficking. *Trends Cell Biol*. 20:196-204.

Lawson, C.D., and A.J. Ridley. 2018. Rho GTPase signaling complexes in cell migration and invasion. *J Cell Biol*. 217:447-457.

Lee, D., and A.L. Goldberg. 2022. 26S proteasomes become stably activated upon heat shock when ubiquitination and protein degradation increase. *Proceedings of the National Academy of Sciences*. 119:e2122482119.

Lee, M.J., and H.G. Dohlman. 2008. Coactivation of G protein signaling by cell-surface receptors and an intracellular exchange factor. *Current biology : CB*. 18:211-215.

Lei, L., J. Bandola-Simon, and P.A. Roche. 2018. Ubiquitin-conjugating enzyme E2 D1 (Ube2D1) mediates lysine-independent ubiquitination of the E3 ubiquitin ligase March-I. *The Journal of biological chemistry*. 293:3904-3912.

Levin, D.E. 2011. Regulation of cell wall biogenesis in Saccharomyces cerevisiae: the cell wall integrity signaling pathway. *Genetics*. 189:1145-1175.

Li, H., Z. Wang, W. Zhang, K. Qian, W. Xu, and S. Zhang. 2016. Fbxw7 regulates tumor apoptosis, growth arrest and the epithelial-to-mesenchymal transition in part through the RhoA signaling pathway in gastric cancer. *Cancer Lett*. 370:39-55.

Li, Y., J. Roberts, Z. AkhavanAghdam, and N. Hao. 2017. Mitogen-activated protein kinase (MAPK) dynamics determine cell fate in the yeast mating response. *The Journal of biological chemistry*. 292:20354-20361.

Lin, C.H., J.A. MacGurn, T. Chu, C.J. Stefan, and S.D. Emr. 2008. Arrestin-Related Ubiquitin-Ligase Adaptors Regulate Endocytosis and Protein Turnover at the Cell Surface. *Cell*. 135:714-725.

Lindquist, S., and E.A. Craig. 1988. The heat-shock proteins. *Annu Rev Genet*. 22:631-677.

Lindstrom, D.L., and D.E. Gottschling. 2009. The mother enrichment program: a genetic system for facile replicative life span analysis in Saccharomyces cerevisiae. *Genetics*. 183:413-422, 411si-413si.

Liu, H., C.A. Styles, and G.R. Fink. 1993. Elements of the yeast pheromone response pathway required for filamentous growth of diploids. *Science*. 262:1741-1744.

Long, R.M., R.H. Singer, X. Meng, I. Gonzalez, K. Nasmyth, and R.P. Jansen. 1997. Mating type switching in yeast controlled by asymmetric localization of ASH1 mRNA. *Science*. 277:383-387.

Longtine, M.S., A. McKenzie, 3rd, D.J. Demarini, N.G. Shah, A. Wach, A. Brachat, P. Philippsen, and J.R. Pringle. 1998. Additional modules for versatile and economical PCR-based gene deletion and modification in Saccharomyces cerevisiae. *Yeast*. 14:953-961.

Lu, A., F. Tebar, B. Alvarez-Moya, C. López-Alcalá, M. Calvo, C. Enrich, N. Agell, T. Nakamura, M. Matsuda, and O. Bachs. 2009. A clathrin-dependent pathway leads to KRas signaling on late endosomes en route to lysosomes. *J Cell Biol*. 184:863-879.

Lu, M.S., and D.G. Drubin. 2020. Cdc42 GTPase regulates ESCRTs in nuclear envelope sealing and ER remodeling. *J Cell Biol*. 219.

Majolée, J., F. Podieh, P.L. Hordijk, and I. Kovačević. 2021. The interplay of Rac1 activity, ubiquitination and GDI binding and its consequences for endothelial cell spreading. *PLoS One*. 16:e0254386.

Martin, S.G. 2015. Spontaneous cell polarization: Feedback control of Cdc42 GTPase breaks cellular symmetry. *Bioessays*. 37:1193-1201.

McClellan, A.J., S.H. Laugesen, and L. Ellgaard. 2019. Cellular functions and molecular mechanisms of non-lysine ubiquitination. *Open Biol*. 9:190147.

McDowell, G.S., and A. Philpott. 2013. Non-canonical ubiquitylation: mechanisms and consequences. *Int J Biochem Cell Biol*. 45:1833-1842.

Miller, K.E., P.J. Kang, and H.-O. Park. 2020. Regulation of Cdc42 for polarized growth in budding yeast. *Microb Cell*. 7:175-189.

Moran, K.D., H. Kang, A.V. Araujo, T.R. Zyla, K. Saito, D. Tsygankov, and D.J. Lew. 2019. Cell-cycle control of cell polarity in yeast. *J Cell Biol*. 218:171-189.

Moreno, D.F., K. Jenkins, S. Morlot, G. Charvin, A. Csikasz-Nagy, and M. Aldea. 2019. Proteostasis collapse, a hallmark of aging, hinders the chaperone-Start network and arrests cells in G1. *eLife*. 8:e48240.

Nassar, N., G.R. Hoffman, D. Manor, J.C. Clardy, and R.A. Cerione. 1998. Structures of Cdc42 bound to the active and catalytically compromised forms of Cdc42GAP. *Nat Struct Biol*. 5:1047-1052.

Ni, M., M. Feretzaki, S. Sun, X. Wang, and J. Heitman. 2011. Sex in Fungi. *Annual Review of Genetics*. 45:405-430.

Olenik, C., K. Aktories, and D.K. Meyer. 1999. Differential expression of the small GTP-binding proteins RhoA, RhoB, Cdc42u and Cdc42b in developing rat neocortex. *Brain Res Mol Brain Res*. 70:9-17.

Onishi, M., N. Ko, R. Nishihama, and J.R. Pringle. 2013. Distinct roles of Rho1, Cdc42, and Cyk3 in septum formation and abscission during yeast cytokinesis. *J Cell Biol*. 202:311-329.

Parr, C.L., R.A. Keates, B.C. Bryksa, M. Ogawa, and R.Y. Yada. 2007. The structure and function of Saccharomyces cerevisiae proteinase A. *Yeast*. 24:467-480.

Perera, R.M., and R. Zoncu. 2016. The Lysosome as a Regulatory Hub. *Annu Rev Cell Dev Biol*. 32:223-253.

Peter, M., A.M. Neiman, H.O. Park, M. van Lohuizen, and I. Herskowitz. 1996. Functional analysis of the interaction between the small GTP binding protein Cdc42 and the Ste20 protein kinase in yeast. *EMBO J*. 15:7046-7059.

Pitoniak, A., C.A. Chavel, J. Chow, J. Smith, D. Camara, S. Karunanithi, B. Li, K.H. Wolfe, and P.J. Cullen. 2015. Cdc42p-interacting protein bem4p regulates the filamentous-growth mitogen-activated protein kinase pathway. *Mol Cell Biol*. 35:417-436.

Pizzirusso, M., and A. Chang. 2004. Ubiquitin-mediated targeting of a mutant plasma membrane ATPase, Pma1-7, to the endosomal/vacuolar system in yeast. *Mol Biol Cell*. 15:2401-2409.

Prabhakar, A., J. Chow, A.J. Siegel, and P.J. Cullen. 2020. Regulation of intrinsic polarity establishment by a differentiation-type MAPK pathway in S. cerevisiae. *J Cell Sci*. 133.

Prabhakar, A., B. González, H. Dionne, S. Basu, and P.J. Cullen. 2021. Spatiotemporal control of pathway sensors and cross-pathway feedback regulate a differentiation MAPK pathway in yeast. *J Cell Sci*. 134.

Prudnikova, T.Y., S.J. Rawat, and J. Chernoff. 2015. Molecular pathways: targeting the kinase effectors of RHO-family GTPases. *Clin Cancer Res*. 21:24-29.

Reidy, M., R. Sharma, S. Shastry, B.-L. Roberts, I. Albino-Flores, S. Wickner, and D.C. Masison. 2014. Hsp40s Specify Functions of Hsp104 and Hsp90 Protein Chaperone Machines. *PLOS Genetics*. 10:e1004720.

Remec Pavlin, M., and J.H. Hurley. 2020. The ESCRTs - converging on mechanism. *J Cell Sci*. 133.

Reymond, N., J.H. Im, R. Garg, F.M. Vega, B. Borda d'Agua, P. Riou, S. Cox, F. Valderrama, R.J. Muschel, and A.J. Ridley. 2012. Cdc42 promotes transendothelial migration of cancer cells through β1 integrin. *J Cell Biol*. 199:653-668.

Ridley, A.J. 2011. Life at the leading edge. *Cell*. 145:1012-1022.

Rose, M., F. Winston, and P. Hieter. 1990. Laboratory course manual for methods in yeast genetics. *Cold Spring Harbor, NY: Cold Spring Harbor Laboratory Press. Open Biol*. 6:14.

Rosenzweig, R., N.B. Nillegoda, M.P. Mayer, and B. Bukau. 2019. The Hsp70 chaperone network. *Nature Reviews Molecular Cell Biology*. 20:665-680.

Rotin, D., O. Staub, and R. Haguenauer-Tsapis. 2000. Ubiquitination and endocytosis of plasma membrane proteins: role of Nedd4/Rsp5p family of ubiquitin-protein ligases. *J Membr Biol*. 176:1-17.

Ryan, O., R.S. Shapiro, C.F. Kurat, D. Mayhew, A. Baryshnikova, B. Chin, Z.Y. Lin, M.J. Cox, F. Vizeacoumar, D. Cheung, S. Bahr, K. Tsui, F. Tebbji, A. Sellam, F. Istel, T. Schwarzmüller, T.B. Reynolds, K. Kuchler, D.K. Gifford, M. Whiteway, G. Giaever, C. Nislow, M. Costanzo, A.C. Gingras, R.D. Mitra, B. Andrews, G.R. Fink, L.E. Cowen, and C. Boone. 2012. Global gene deletion analysis exploring yeast filamentous growth. *Science*. 337:1353-1356.

Saarikangas, J., F. Caudron, R. Prasad, D.F. Moreno, A. Bolognesi, M. Aldea, and Y. Barral. 2017. Compartmentalization of ER-Bound Chaperone Confines Protein Deposit Formation to the Aging Yeast Cell. *Current Biology*. 27:773-783.

Saito, H. 2010. Regulation of cross-talk in yeast MAPK signaling pathways. *Curr Opin Microbiol*. 13:677-683.

Saito, H., and F. Posas. 2012. Response to hyperosmotic stress. *Genetics*. 192:289-318.

Sala, A.J., L.C. Bott, and R.I. Morimoto. 2017. Shaping proteostasis at the cellular, tissue, and organismal level. *J Cell Biol*. 216:1231-1241.

Samant, R.S., C.M. Livingston, E.M. Sontag, and J. Frydman. 2018. Distinct proteostasis circuits cooperate in nuclear and cytoplasmic protein quality control. *Nature*. 563:407-411.

Santra, M., K.A. Dill, and A.M.R. de Graff. 2019. Proteostasis collapse is a driver of cell aging and death. *Proc Natl Acad Sci U S A*. 116:22173-22178.

Settembre, C., A. Fraldi, D.L. Medina, and A. Ballabio. 2013. Signals from the lysosome: a control centre for cellular clearance and energy metabolism. *Nature Reviews Molecular Cell Biology*. 14:283-296.

Sieber, B., J.M. Coronas-Serna, and S.G. Martin. 2022. A focus on yeast mating: From pheromone signaling to cell-cell fusion. *Seminars in Cell & Developmental Biology*.

Sikorski, R.S., and P. Hieter. 1989. A system of shuttle vectors and yeast host strains designed for efficient manipulation of DNA in Saccharomyces cerevisiae. *Genetics*. 122:19-27.

Simon, M.N., C. De Virgilio, B. Souza, J.R. Pringle, A. Abo, and S.I. Reed. 1995. Role for the Rho-family GTPase Cdc42 in yeast mating-pheromone signal pathway. *Nature*. 376:702-705.

Slaughter, B.D., S.E. Smith, and R. Li. 2009. Symmetry breaking in the life cycle of the budding yeast. *Cold Spring Harb Perspect Biol*. 1:a003384-a003384.

Sommer, T., A. Weber, and E. Jarosch. 2014. Rsp5/Nedd4 clears cells of heat-damaged proteins. *Nat Cell Biol*. 16:1130-1132.

Sprague, G.F., Jr., L.C. Blair, and J. Thorner. 1983. Cell interactions and regulation of cell type in the yeast Saccharomyces cerevisiae. *Annu Rev Microbiol*. 37:623-660.

Strochlic, T.I., B.C. Schmiedekamp, J. Lee, D.J. Katzmann, and C.G. Burd. 2008. Opposing activities of the Snx3-retromer complex and ESCRT proteins mediate regulated cargo sorting at a common endosome. *Mol Biol Cell*. 19:4694-4706.

Strohacker, L.K., D.R. Mackay, M.A. Whitney, G.C. Couldwell, W.I. Sundquist, and K.S. Ullman. 2021. Identification of abscission checkpoint bodies as structures that regulate ESCRT factors to control abscission timing. *eLife*. 10:e63743.

Svensmark, J.H., and C. Brakebusch. 2019. Rho GTPases in cancer: friend or foe? *Oncogene*. 38:7447-7456.

Swatek, K.N., and D. Komander. 2016. Ubiquitin modifications. *Cell Res*. 26:399-422.

Tait, S.W., E. de Vries, C. Maas, A.M. Keller, C.S. D'Santos, and J. Borst. 2007. Apoptosis induction by Bid requires unconventional ubiquitination and degradation of its N-terminal fragment. *J Cell Biol*. 179:1453-1466.

Tamehiro, N., H. Oda, M. Shirai, and H. Suzuki. 2015. Overexpression of RhoH Permits to Bypass the Pre-TCR Checkpoint. *PLOS ONE*. 10:e0131047.

Tolliday, N., L. VerPlank, and R. Li. 2002. Rho1 directs formin-mediated actin ring assembly during budding yeast cytokinesis. *Current biology : CB*. 12:1864-1870.

Ukmar-Godec, T., P. Fang, A. Ibáñez de Opakua, F. Henneberg, A. Godec, K.T. Pan, M.S. Cima-Omori, A. Chari, E. Mandelkow, H. Urlaub, and M. Zweckstetter. 2020. Proteasomal degradation of the intrinsically disordered protein tau at single-residue resolution. *Sci Adv*. 6:eaba3916.

Vanneste, M., C.R. Feddersen, A. Varzavand, E.Y. Zhu, T. Foley, L. Zhao, K.H. Holt, M. Milhem, R. Piper, C.S. Stipp, A.J. Dupuy, and M.D. Henry. 2020. Functional Genomic Screening Independently Identifies CUL3 as a Mediator of Vemurafenib Resistance via Src-Rac1 Signaling Axis. *Front Oncol*. 10:442.

Vietri, M., M. Radulovic, and H. Stenmark. 2020. The many functions of ESCRTs. *Nature Reviews Molecular Cell Biology*. 21:25-42.

Visintin, R., S. Prinz, and A. Amon. 1997. CDC20 and CDH1: a family of substrate-specific activators of APC-dependent proteolysis. *Science*. 278:460-463.

Wang, F., R. Gómez-Sintes, and P. Boya. 2018. Lysosomal membrane permeabilization and cell death. *Traffic*. 19:918-931.

Wang , X., R.A. Herr , W.-J. Chua , L. Lybarger , E.J.H.J. Wiertz , and T.H. Hansen 2007. Ubiquitination of serine, threonine, or lysine residues on the cytoplasmic tail can induce ERAD of MHC-I by viral E3 ligase mK3. *Journal of Cell Biology*. 177:613-624.

Wang, Y., S. Fang, G. Chen, R. Ganti, T.A. Chernova, L. Zhou, D. Duong, H. Kiyokawa, M. Li, B. Zhao, N. Shcherbik, Y.O. Chernoff, and J. Yin. 2021. Regulation of the endocytosis and prion-chaperoning machineries by yeast E3 ubiquitin ligase Rsp5 as revealed by orthogonal ubiquitin transfer. *Cell Chem Biol*. 28:1283-1297.e1288.

Wei, J., R.K. Mialki, S. Dong, A. Khoo, R.K. Mallampalli, Y. Zhao, and J. Zhao. 2013. A new mechanism of RhoA ubiquitination and degradation: roles of SCF(FBXL19) E3 ligase and Erk2. *Biochim Biophys Acta*. 1833:2757-2764.

Winzeler, E.A., D.D. Shoemaker, A. Astromoff, H. Liang, K. Anderson, B. Andre, R. Bangham, R. Benito, J.D. Boeke, H. Bussey, A.M. Chu, C. Connelly, K. Davis, F. Dietrich, S.W. Dow, M. El Bakkoury, F. Foury, S.H. Friend, E. Gentalen, G. Giaever, J.H. Hegemann, T. Jones, M. Laub, H. Liao, N. Liebundguth, D.J. Lockhart, A. Lucau-Danila, M. Lussier, N. M'Rabet, P. Menard, M. Mittmann, C. Pai, C. Rebischung, J.L. Revuelta, L. Riles, C.J. Roberts, P. Ross-MacDonald, B. Scherens, M. Snyder, S. Sookhai-Mahadeo, R.K. Storms, S. Véronneau, M. Voet, G. Volckaert, T.R. Ward, R. Wysocki, G.S. Yen, K. Yu, K. Zimmermann, P. Philippsen, M. Johnston, and R.W. Davis. 1999. Functional characterization of the S. cerevisiae genome by gene deletion and parallel analysis. *Science*. 285:901-906.

Woods, B., H. Lai, C.-F. Wu, T.R. Zyla, N.S. Savage, and D.J. Lew. 2016a. Parallel Actin-Independent Recycling Pathways Polarize Cdc42 in Budding Yeast. *Current biology : CB*. 26:2114-2126.

Woods, B., H. Lai, C.F. Wu, T.R. Zyla, N.S. Savage, and D.J. Lew. 2016b. Parallel Actin-Independent Recycling Pathways Polarize Cdc42 in Budding Yeast. *Current biology : CB*. 26:2114-2126.

Woods, B., and D.J. Lew. 2019. Polarity establishment by Cdc42: Key roles for positive feedback and differential mobility. *Small GTPases*. 10:130-137.

Yoshida, A., D. Wei, W. Nomura, S. Izawa, and Y. Inoue. 2012. Reduction of glucose uptake through inhibition of hexose transporters and enhancement of their endocytosis by methylglyoxal in Saccharomyces cerevisiae. *The Journal of biological chemistry*. 287:701-711.

Yoshida, S., S. Bartolini, and D. Pellman. 2009. Mechanisms for concentrating Rho1 during cytokinesis. *Genes Dev*. 23:810-823.

Zhang, Y., J. Li, X.N. Lai, X.Q. Jiao, J.P. Xiong, and L.X. Xiong. 2019. Focus on Cdc42 in Breast Cancer: New Insights, Target Therapy Development and Non-Coding RNAs. *Cells*. 8.

Zhou, F., Z. Wu, M. Zhao, R. Murtazina, J. Cai, A. Zhang, R. Li, D. Sun, W. Li, L. Zhao, Q. Li, J. Zhu, X. Cong, Y. Zhou, Z. Xie, V. Gyurkovska, L. Li, X. Huang, Y. Xue, L. Chen, H. Xu, H. Xu, Y. Liang, and N. Segev. 2019. Rab5-dependent autophagosome closure by ESCRT. *J Cell Biol*. 218:1908-1927.

Ziman, M., J.M. O'Brien, L.A. Ouellette, W.R. Church, and D.I. Johnson. 1991. Mutational analysis of CDC42Sc, a Saccharomyces cerevisiae gene that encodes a putative GTP-binding protein involved in the control of cell polarity. *Mol Cell Biol*. 11:3537-3544.

TABLES

Table 1. Yeast strains.

Name	Genotype	Reference
PC313[a]	*MAT***a** *ura3-52*	(Liu et al., 1993)
PC538[a]	*MAT***a** *ste4 FUS1-lacZ FUS1-HIS3 ura3-52*	(Cullen et al., 2004)
PC673[a]	*MAT***a** *ste4 FUS1-lacZ FUS1-HIS3 ura3-52 ste20::kanMX6*	(Cullen et al., 2004)
PC986[b]	*MAT*α *his3Δ0, leu2Δ0, met15Δ0, ura3Δ0*	(Winzeler et al., 1999)
PC999[a]	*MAT***a** *ste4 FUS1-lacZ FUS1-HIS3 ura3-52 Msb2-HA*	(Cullen et al., 2004)
PC1894[a]	*MAT***a** *ste4 FUS1-lacZ FUS1-HIS3 ura3-52 leu2::HYG*	(Pitoniak et al., 2015)
PC3063[b]	*MAT*α *his3Δ0, leu2Δ0, met15Δ0, ura3Δ0 pep4::kanMX6*	(Winzeler et al., 1999)
PC3288[b]	*MAT*α *ura3-52 his3-200 trp1-901 lys2-801 suc2-p leu2-3*	(Strochlic et al., 2008)
PC3154[a]	*MAT***a** *ste4 FUS1-lacZ FUS1-HIS3 ura3-52 Msb2-HA pep4:KLURA*	(Adhikari et al., 2015b)
PC3290[b]	*MAT*α *ura3-52 his3-200 trp1-901 lys2-801 suc2-p leu2-3 rsp5-1*	(Strochlic et al., 2008)
PC3391[a]	*MAT***a** *ste4 FUS1-lacZ FUS1-HIS3 ura3-52 rga1::NAT*	(Pitoniak et al., 2015)
PC3862[a]	*MAT***a** *ste4 FUS1-lacZ FUS1-HIS3 ura3-52 ste11::NAT*	(Pitoniak et al., 2015)
PC5851[b]	*MAT***a** *ura3-52 his3-200 ade2-101 his3-200 leu2-1*	(Ghislain et al., 1993)
PC5852[b]	*MAT***a** *ura3-52 his3-200 ade2-101 his3-200 leu2-1 cim3-1*	(Ghislain et al., 1993)
PC5024[a]	*MAT***a** *ura3-52 ste11::NAT*	(Pitoniak et al., 2015)
PC6016[a,c]	*MAT***a** *can1Δ::Ste2pr-spHIS5 lyp1Δ::Ste3pr-LEU2 his3::hisG leu2Δ0 ura3Δ0*	(Ryan et al., 2012)
PC6102[a]	*MAT***a** *ste4 FUS1-lacZ FUS1-HIS3 ura3-52 tec1::NAT*	(Chavel et al., 2014)
PC6539[a]	*MAT***a** *ste4 FUS1-lacZ FUS1-HIS3 ura3-52 cdc42::NAT* pRS316-GFP-linker-CDC42	(González and Cullen, 2022)
PC6591[a]	*MAT***a** *ura3-5 leu2*	(González and Cullen, 2022)
PC6810[a]	*MAT***a** *ura3-52 leu2 ssk1*	(González and Cullen, 2022)
PC6604[a]	*MAT***a** *ura3-52 leu2 ssk1 ste11::NAT*	(González and Cullen, 2022)
PC6684[a]	*MAT***a** *ura3-52 leu2 ssk1 cdc42::NAT* pRS316-GFP-linker-CDC42	(Basu et al., 2020)
PC7034[a]	*MAT***a** *ste4 FUS1-lacZ FUS1-HIS3 ura3-52 gic1::kanMX6*	(Prabhakar et al., 2020)
PC7043[a]	*MAT***a** *ste4 FUS1-lacZ FUS1-HIS3 ura3-52 gic2::NAT*	(Prabhakar et al., 2020)
PC7044[a]	*MAT***a** *ste4 FUS1-lacZ FUS1-HIS3 ura3-52 gic1::kanMX6 gic2:: NAT*	(Prabhakar et al., 2020)
PC7086[a]	*MAT***a** *ste4 FUS1-lacZ FUS1-HIS3 ura3-52 bni1::NAT*	(González and Cullen, 2022)
PC7179[a]	*MAT***a** *ura3-52 leu2 ssk1 bem4::NAT*	(González and Cullen, 2022)
PC7502[a]	*MAT***a** *ste4 FUS1-lacZ FUS1-HIS3 ura3-52 rdi1::NAT*	(González and Cullen, 2022)
PC7546[a]	*MAT***a** *can1Δ::Ste2pr-spHIS5 lyp1Δ::Ste3pr-LEU2 his3::hisG leu2Δ0 ura3Δ0 vps27::kanMX6*	(Ryan et al., 2012)
PC7547[a]	*MAT***a** *can1Δ::Ste2pr-spHIS5 lyp1Δ::Ste3pr-LEU2 his3::hisG leu2Δ0 ura3Δ0 vps23::kanMX6*	(Ryan et al., 2012)
PC7548[a]	*MAT***a** *can1Δ::Ste2pr-spHIS5 lyp1Δ::Ste3pr-LEU2 his3::hisG leu2Δ0 ura3Δ0 vps22::kanMX6*	(Ryan et al., 2012)
PC7549[a]	*MAT***a** *can1Δ::Ste2pr-spHIS5 lyp1Δ::Ste3pr-LEU2 his3::hisG leu2Δ0 ura3Δ0 vps32::kanMX6*	(Ryan et al., 2012)
PC7550[a]	*MAT***a** *can1Δ::Ste2pr-spHIS5 lyp1Δ::Ste3pr-LEU2 his3::hisG leu2Δ0 ura3Δ0 vps4::kanMX6*	(Ryan et al., 2012)
PC7616[a]	*MAT***a** *ste4 FUS1-lacZ FUS1-HIS3 ura3-52 ydj1::NAT*	(González and Cullen, 2022)
PC7619[a]	*MAT***a** *ura3-52 leu2 ssk1 ydj1::NAT*	(González and Cullen, 2022)
PC7621[a]	*MAT***a** *ste4 FUS1-lacZ FUS1-HIS3 ura3-52 ssa1::NAT*	(González and Cullen, 2022)
PC7623[a]	*MAT***a** *ura3-52 leu2 ssk1 ssa1::NAT*	(González and Cullen, 2022)
PC7657[b]	*MAT*α *his3Δ0, leu2Δ0, met15Δ0, ura3Δ0 ydj1::kanMX6*	(Winzeler et al., 1999)
PC7826[a]	*MAT***a** *ste4 FUS1-lacZ FUS1-HIS3 ura3-52 rsp5-1::NAT tec1::HYG*	(González and Cullen, 2022)
PC7700[c,a]	*MAT***a** *can1Δ::Ste2pr-spHIS5 lyp1Δ::Ste3pr-LEU2 his3::hisG leu2Δ0 ura3Δ0 ssa1:: kanMX6*	(Ryan et al., 2012)
PC7713[b]	*MAT***a** *ade2::hisG his3 leu2 lys2 ura3Δ0 trp1Δ63 hoΔ::SCW11pr-Cre-EBD78-NatMX loxP-UBC9-loxP-LEU2 loxP-CDC20-intron-loxP-HPHMX trp1Δ63::SCW11pr-Cre-EBD78-KanMX4*	(Moreno et al., 2019)

a. Strains are Σ1278b background.
b. S288c background.
c. Strains from an ordered deletion collection described in (Ryan et al., 2012) were also used.

Table 2. Plasmids used in the study.

Name	Description	Reference
PC2207	pRS316	(Sikorski and Hieter, 1989)
PC2582	MSB2-HA-GFP	(Adhikari et al., 2015a)
PC6455	pRS306-GFP-linker-CDC42 (pDLB3609)	(Irazoqui et al., 2003)
PC6454	pRS316-GFP-linker-CDC42	(Basu et al., 2020)
PC6457	pRS315-GFP-linker-CDC42	(Basu et al., 2020)
PC7349	pRS316-GAL1-GFP-Cdc42p	This study
PC7350	pRS316-GFP-linker-CDC42 (C188S)	(González and Cullen, 2022)
PC7354	pRS316-GFP-linker-CDC42 *ura3*::*kanMX6*	(Prabhakar et al., 2021)
PC7455	pRS316-GFP-linker-CDC42 (D57Y)	(González and Cullen, 2022)
PC7458	pRS316-GFP-linker-CDC42 (Q61L)	(González and Cullen, 2022)
PC7504	pRS316-GFP-linker-CDC42 (K5R, K16R)	This study
PC7506	pRS316-GFP-linker-CDC42 (K16R, K166R)	This study
PC7507	pRS316-GFP-linker-CDC42 (K5R, K16R. K94R, K96R)	This study
PC7508	pRS316-GFP-linker-CDC42 (K94R, K96R)	This study
PC7509	pRS316-GFP-linker-CDC42 (K5R, K16R, K94R, K96R, K123R, K128R, K166R)	This study
PC7511	pRS316-GFP-linker-CDC42 (K150R, K153R)	(González and Cullen, 2022)
PC7512	pRS316-GFP-linker-CDC42 (K16R, K150R, K153R, K166R)	This study
PC7513	pRS316-GFP-linker-CDC42 (K5R, K16R, K94R, K96R, K123R, K128R, K150R, K153R, K166R)	This study
PC7518	pRS316-GFP-linker-CDC42 (K166R)	This study
PC7520	pRS316-GFP-linker-CDC42 (K183R, K184R, K186R, K187R)	This study
PC7521	pRS316-GFP-linker-CDC42 (13KR; K5R, K16R, K94R, K96R, K123R, K128R, K150R, K153R, K166R, K183R, K184R, K186R, K187R)	This study
PC7571	p6xHis-linker-CDC42	This study
PC7572	p6xHis-linker-CDC42 (K5R, K16R, K94R, K96R, K123R, K128R, K150R, K153R, K166R, K183R, K184R, K186R, K187R)	This study
PC7633	pRS316-GFP-linker-CDC42 (12KR; K5R, K94R, K96R, K123R, K128R, K150R, K153R, K166R, K183R, K184R, K186R, K187R)	This study
PC7635	pRS316-GFP-linker-CDC42 (K5R, K123R, K128R, K166R)	(González and Cullen, 2022)
PC7636	pRS316-GFP-linker-CDC42 (K5R, K94R, K96R)	(González and Cullen, 2022)
PC7637	pRS316-GFP-linker-CDC42 (K5R, K150R, K153R, K166R)	(González and Cullen, 2022)
PC7638	pRS316-GFP-linker-CDC42 (Q61L, K166R)	(González and Cullen, 2022)
PC7651	pRS316-GFP-linker-CDC42 (K5R, Q61L, K123R, K128R, K166R)	(González and Cullen, 2022)
PC7654	pRS316-GFP-linker-CDC42 (K5R, Q61L, K94R, K96R)	(González and Cullen, 2022)
PC7662	pRS316-GFP-linker-CDC42 (Q61L, K94R, K96R)	(González and Cullen, 2022)
PC7664	pRS316-GFP-linker-CDC42 (Q61L, K150R, K153R)	(González and Cullen, 2022)
PC7665	pRS316-GFP-linker-CDC42 (Q61L, K183R, K184R, K186R, K87R)	(González and Cullen, 2022)
PC7666	pRS316-GFP-linker-CDC42 (K5R, Q61L, K94R, K96R, K123R, K128R, K150R, K153R, K166R, K183R, K184R, K186R, K187R)	(González and Cullen, 2022)
PC7667	pRS316-GFP-linker-CDC42 (K5R, Q61L, K150R, K153R, K166R)	(González and Cullen, 2022)
PC7668	pRS316-GFP-linker-CDC42 (G12V)	(González and Cullen, 2022)
PC7697	pRS315-GFP-linker-CDC42 (K16R)	(González and Cullen, 2022)
PC7830	pRS313-CDC3-mCherry::HYG	This study

Table 3. Primers used in the study.

Name	Sequence (5′-3′)	Approach
K5R K16R F1	*TGCGGCCGCGCACCACCACGACGACTAGTACACCCACAAACGCTAAGGTGTGTT GTTGTCGGTGATGGTGCTGTTGGGAGAACGTGCCTTCTAATCTCCTATA*	HR[b]
K123R K128R R1	*AACCTTGTTCTGATGTAATCGGACGTAATCTTTGTCTTTGCAACCTCTCGATGATT ACCCTGTCATCCCTTAGATCAATCTGCG*	HR[b]
K94R K96R R1	*TGGTACACCTGGACAATGGTGATGTACTTCAGGGAACCATCTTTCTCTAACGTTTT CAAAAGAGGGTGGGGA*	HR[b]
K150R K153R R1	*CAAACCGCGTTGTGTTAGTGCCGAACACTCGACATATCTTACTGCTCTCAGTTCT CTTGCTAACCTGGA*	HR[b]
K183R K184R K186R K187R F1	*TTGGAGCCTCCTGTTATCAGGAGAAGTAGAAGATGTACAATTTTGTAGTC*	SDM[a]
K183R K184R K186R K187R R1	*GACTACAAAATTGTACATCTTCTACTTCTCCTGATAACAGGAGGCTCCAA*	SDM[a]
GFP by His6x F1	*AAATAAACGTATTAGGTCTTCCACAAAATGAGCGGCCGCATGCATCATCATCATC ATCATGGATCCTGCGGCCGCGCACCACCACGACGACTAGTACACCCA*	HR[b]
GFP by His6x R1	*AAATAAACGTATTAGGTCTTCCACAAAATGAGCGGCCGCATG*	HR[b]

[a]SDM: Site Directed Mutagenesis
[b]HR: Homologous Recombination

FIGURES LEGENDS

Figure 1. Degradation of Cdc42p is induced at 37ºC in a chaperone- and Rsp5p-dependent manner. A) Top, Cdc42p levels in wild-type (WT, Σ1278b, PC538) cells incubated for 4h at 30ºC and shifted to 37°C for the indicated time points. Anti-Cdc42p and anti-Pgk1 antibodies were used. Bottom, wild-type cells expressing GFP-Cdc42p (PC6454) were grown at 30ºC for 5 h and shifted to 37ºC, samples were analyzed at the indicated time points. Anti-GFP and anti-Pgk1 antibodies were used. **B)** Cdc42p levels in wild-type (WT) cells grown in media containing 25 µg/ml of cycloheximide at 30°C and analyzed by immunoblotting at the indicated time points. See Fig. 1A for details. **C)** Relative protein quantification of Cdc42p at 30°C (panel 1B, black) and at 37°C (panel 1A, yellow) to account for the turnover rates. Error bars represent the S.D from two biological replicates. Dashed line indicates the half-life of the protein. Data were analyzed by one-way ANOVA and Tukey's multiple comparison test. **D)** Cdc42p levels in wild-type (WT, S288C, PC986) cells and the *ydj1*Δ (PC7657) mutant grown at 30°C for 5 h (30°C) and shifted to 37°C for 2 h (37°C). Anti-Cdc42p and anti-Pgk1 antibodies were used. Bottom, graph represents quantification of the relative levels of Cdc42 compared to Pgk1 from three biological replicates, n = 3. Data were analyzed by one-way ANOVA followed by a Tukey's multiple comparison test. **E)** Cdc42p levels in wild-type (WT, Σ1278b, PC6016) cells and the *ssa1*Δ (PC7700) mutant grown at 30°C for 5 h (30°C) or shifted to 37°C for 2 h (37°C). See Fig. 1D for details. **F)** Levels of GFP-Cdc42p (PC6454) expressed in wild-type (WT, S288C, PC3288) and *rsp5-1* (PC3290) cells incubated 5 h at 30ºC (30ºC) and 2h at 37ºC (37ºC). See Fig. 1D for details. Same results were shown in (González and Cullen, 2022).

Figure 2. Lysines residues required for Cdc42p degradation at 37ºC. A) The yeast Cdc42p protein sequence was overlaid onto the crystal structure of human Cdc42p. Yellow refers to lysines involved in Cdc42p turnover at 37°C, red refers to lysines involved GTP-Cdc42p (González and Cullen, 2022) turnover and green indicates lysine involved in protein stability. **B)** 37ºC, GFP-Cdc42p levels of wild-type cells (WT, Σ1278b, PC538) expressing GFP-Cdc42p (PC6454), GFP-Cdc42p^{K5R,K94R,K96R} (PC7636), GFP-Cdc42p^{K166R} (PC7518), GFP-Cdc42p^{PB} (PB: K183R, K184R, K186R, K187R; PC7520) grown and at 30°C for 5 h and shifted to 37°C for 2 h. Q61L, GFP-Cdc42p levels of wild-type cells expressing GFP-Cdc42p^{Q61L} (PC7458), GFP-Cdc42p$^{Q61L+TD}$ (TD: K5R, K94R, K96R; PC7654), GFP-Cdc42p^{Q61L,K166R} (PC7638), GFP-Cdc42p$^{Q61L+PB}$ (PC7665) grown and at 30°C for 5 h and shifted to 37°C for 2 h. See Fig. 1D for details. **C)** Heat map shows protein levels of indicated lysine substitutions of GFP-Cdc42p in wild-type cells. First row (37ºC) refers to protein levels of Cdc42p containing the indicated lysine substitutions in strains grown at 37ºC, second row (GTP-Cdc42) refers to protein levels of GTP-Cdc42 containing Q61L and the indicated lysine substitutions in strains grown at 30ºC. Color code represents the relative fold change of GFP-Cdc42p lysine substitutions compared to wild-type GFP-Cdc42p. Grey color indicates lysine substitutions to arginines in GFP-Cdc42p. Colors of alleles are described in **Fig. 2A**. Some data comes from (González and Cullen, 2022).

Figure 3. Cdc42p can be degraded by the vacuole in an ESCRT-dependent manner. A) Wild-type (WT, S288C, PC5851) cells and the *cim3-1* (PC5852) mutant expressing GFP-Cdc42p (PC6454) grown at 30ºC for 5 h (30ºC) and shifted to 37ºC for 2 h (37ºC). See Fig. 1D for details. **B)** Wild-type cells (WT, Σ1278b, PC999) and the *pep4*Δ mutant (PC3154) expressing GFP-Cdc42p (PC7354) grown at 37ºC during the indicated time points. Bottom graph represents the

quantification of GFP-Cdc42p levels compared to Pgk1p. Dashed line indicates the half-life of the protein. Error bars represents S. D. from two biological replicates. **C)** Wild-type cells (WT, PC986) and the *pep4*Δ (PC3063) mutant expressing GFP-Cdc42p were grown at 30ºC for 5 h. **D)** Wild-type cells (WT, Σ1278b, PC6016) and the *vps22*Δ mutant (PC7548) expressing GFP-Cdc42p (PC6454) grown at 37ºC during the indicated time points. Dashed line indicates the half-life of the protein. See Fig. 3D for details. **E)** Wild-type cells and the *vps22*Δ mutant expressing GFP-Cdc42p (PC6454) were incubated and 30ºC for 5h (30ºC) and shifted to 37ºC, cells were visualized at the indicated time points. Bar, 5µm. **F)** Relative fluorescence quantification of same cells. Data were analyzed by one-way ANOVA followed by Tukey's multiple comparison test, n = 25, S.D. represents the standard deviation.

Figure 4. **Cdc42p unable to bind to membranes is not recruited in the ESCRT-vacuole pathway. A)** Fluorescence microscopy of wild-type cells and the *vps22*Δ mutant expressing GFP-Cdc42p^{C188S} (PC7350) grown to mid-log phase at 30ºC. Bar, 5µm. **B)** Immunoblot analysis of wild-type cells (Σ1278b, PC538) expressing GFP-Cdc42p and GFP-Cdc42p^{C188S}. **C)** GFP-Cdc42p refers to GFP-Cdc42p levels compared to Pgk1p from two biological replicates. GFP refers to free GFP divided by GFP-Cdc42p intensity from two biological replicates. Error bars represent the standard deviation, and t-test was used to generate p-values.

Figure 5. GTP-Cdc42p is not degraded by the ESCRT-vacuole pathway. A) Fluorescence microscopy of wild-type cells (WT, Σ1278b, PC6016) expressing Msb2p-GFP (PC2582), GFP-Cdc42p (PC6454) or GFP-Cdc42p^{Q61L} (PC7458) grown for 5 h at 30ºC and stained with FM4-64

dye. Arrows indicate colocalization of GFP-Cdc42p and FM4-64. Bar, 5µm. **B)** Fluorescence microscopy of wild-type cells (PC6016) and the indicated ESCRT mutants expressing Msb2p-GFP, GFP-Cdc42p, or GFP-Cdc42p^{Q61L} grown for 5 h at 30ºC. Bar, 5µm. **C)** Wild-type cells (WT, S288C, PC986) and the *pep4*Δ (PC3063) mutant expressing GFP-Cdc42p^{Q61L} grown at 30ºC for 5 h (30ºC) and shifted to 37ºC for 2 h (37ºC). See Fig. 1D for details. **D)** Levels of GFP-Cdc42p^{Q61L} in WT cells incubated at 37ºC for the indicates times. Cdc42/Pgk1 ratio refers to relative levels of GFP-Cdc42p^{Q61L} to Pgk1p. **E)** Wild-type cells and the *vps22*Δ mutant expressing GFP-Cdc42p^{Q61L} were incubated and 30ºC for 5h (30ºC) and shifted to 37ºC, cells were visualized at the indicated time points. Bar, 5µm.

Figure 6. The impact of Cdc42p turnover on MAPK pathways-dependent phenotypes and cell polarity. A) Halo formation in response to α-factor of wild-type (WT, S288C, PC896) cells and the *ydj1*Δ (PC7657) mutant. Cells grown for 16 h were spread on SD media where 6 µM α-factor was spotted on the top to study cell cycle arrest, plates were incubated for 48 h at the indicated temperature. **B)** Relative halo size of same cells examined in panel 3A. Data were analyzed by one-way ANOVA followed by a Tukey's multiple comparison test, n = 4, Error bars refer to S.D. **C)** Halo formation in response to α-factor of wild-type (WT, Σ1278b, PC6810) cells and indicated *CDC42* alleles. Cells grown for 16 h were spread on YEPD media where 6 µM α-factor was spotted to induce pheromone-dependent cell cycle arrest, plates were incubated for 48 h at the indicated temperature. Wild-type cells, Cdc42p^{PB}, and Cdc42p^{K163R,K166R} alleles were grown on YPD for 48h at 34ºC. **D)** Relative halo size is shown for the same cells examined in panel 3C. Data were analyzed by one-way ANOVA followed by a Tukey's multiple comparison test, n= 4, Error bars refer to standard deviation. **E)** Halo formation in WT cells expressing GFP-

Cdc42p (Cdc42), GFP-Cdc42p^{Q61L} (Q61L), and GFP-Cdc42p$^{K5R;\ Q61L;\ K94R;\ K96R}$ (Q61L+TD) in response to two concentrations of a-factor, 1.6 µM and 6 µM. Cells were incubated for 48 h at 37ºC. **F~~D~~)** Bottom, data were analyzed by one-way ANOVA followed by a Tukey's multiple comparison test, n= 4, Error bars refer to standard deviation. **G~~E~~)** Serial dilutions of wild-type cells and *CDC42* alleles grown at 30ºC and 34ºC for 3 days. **H~~F~~)** Wild-type cells, Cdc42p^{K183A,K184A,K186A,K187A} (PB), and Cdc42p^{K163R,K166R} alleles expressing Cdc3-mCherry (PC7830) were grown on YPED for 12 h at 34ºC and visualized by confocal microscopy. Arrows indicate accumulation of multiple septin rings in the same cell. Bar, 5µm.

Figure 7. Analysis of the K16R mutation: impact on Cdc42p levels and aggregate formation. **A)** Wild-type cells (WT, Σ1278b, PC538) expressing GFP-Cdc42p (No change, PC6454), GFP-Cdc42p^{K94R,K96R} (PC7508), GFP-Cdc42p^{K166R} (PC7518), GFP-Cdc42p^{K150R,K153R} (PC7511), GFP-Cdc42p^{K183R,K184R,K186R,K187R} (PC7520), GFP-Cdc42p^{K5R,K16R} (PC7504), GFP-Cdc42p ^{K5R,K16R,K94R,K96R} (PC7507), GFP-Cdc42p^{K5R,K16R,K94R,K96R,K123R,K128R,K153R,K166R} (PC7513), and GFP-Cdc42p$^{K5R,K16R,K94R,K96R,K123R,K128R,K150R,K153R;,K166R,K183R,K184R,K186R,K187R}$ (13KR; PC7521) grown to mid-log phase at 30ºC. **B)** Quantification of GFP-Cdc42p levels from three biological replicates, n= 3, analyzed by one-way ANOVA and Tukey's multiple comparison test. Error bars refers to standard deviation. **C)** Heat map showing aggregates resembling pattern of the indicated alleles expressed in *cim3-1* cells in wild-type cells grown to mid-log phase at 30ºC (Levels). First row **(**levels) indicates the relative protein levels of the indicated lysine substitutions respect wild-type Cdc42p. Second row (Agg) refers to lysines substitutions that showed aggregates resembling pattern. **D)** WT and *cim3-1* mutant cells expressing GFP-Cdc42^{13KR} grown to mid log phase at 30ºC and shifted for 1h to 37ºC. **E)** *cim3-1* mutant cells expressing Hisx6-Cdc42 (No Change;

PC7571) and Hisx6-Cdc42 ^{K5R,K16R,K94R,K96R,K123R,K128R,K150R,K153R,K166R,K183R,K184R,K186R,K187R} (13KR; PC7572) grown to mid-log phase at 30ºC. **F)** Confocal microscopy of *cim3-1* cells expressing GFP-Cdc42p (No change), GFP-Cdc42^{K5R,K16R,K94R,K96R,K123R,K128R,K150R,K153R,K166R,K183R,K184R,K186R,K187R} (13KR), GFP-Cdc42pK16R (PC7607), and GFP-Cdc42^{K5R,K94R,K96R,K123R,K128R,K150R,K153R,K166R,K183R,K184R,K186R,K187R} (12KR; PC7633) grown at 37ºC for 2 h. Bar, 5µm. **F)** Confocal microscopy of *cim3-1* cells expressing GFP-Cdc42p (No change), GFP-Cdc42^{K5R,K16R,K94R,K96R,K123R,K128R,K150R,K153R,K166R,K183R,K184R,K186R,K187R} (13KR), GFP-Cdc42pK16R (PC7607), and GFP-Cdc42^{K5R,K94R,K96R,K123R,K128R,K150R,K153R,K166R,K183R,K184R,K186R,K187R} (12KR; PC7633) grown at 37ºC for 2 h. Bar, 5µm. **G)** Localization of same GFP-Cdc42p alleles indicated in panel 7A expressed in *cim3-1* mutant (PC5852) cells incubated at 37ºC for 2h. Bar, 5µm

Figure 8. Cdc42p aggregates mostly localized in aging cells. A) Left, fluorescence microscopy of wild-type cells expressing pP_{GAL1}-GFP-linker-*CDC42P* grown for 8 h in YEP-GAL media. Bar, 5 µm. Right, relative quantification of the aggregates area from more that 50 cells. **B)** Time-lapse confocal microscopy of wild-type cells and the the *cim3-1* mutant (PC5852) expressing GFP-Cdc42p^{K16R} (K16R) and grown at 37ºC. Bar, 5µm. **C)** Fluorescence microscopy of MEP cells (PC7713) expressing GFP-Cdc42p (PC6454) and stained with WGA-alexa-647 grown for 48h at 30ºC. Arrows indicate GFP-Cdc42p aggregates. Bar, 5µm. **D)** Relative quantification of GFP-Cdc42p levels at the plasma membrane of MEP cells grown for 48h at 30ºC. p-values were obtained using Mann-Whitney U test, n > 25 cells.

Figure 9. Mechanisms underlying Cdc42p turnover regulation in yeast. At 37ºC (left panels, yellow), Cdc42p is degraded by the chaperones Ydj1p (HSP40) and Ssa1p (HSP70), and the NEDD4 ubiquitin ligase Rsp5p. Cdc42p turnover at 37ºC requires amino acid residues K166 and lysines at the C-terminus of the protein (K183, K184, K186, K187, or PB). Turnover of Cdc42p at 37˚C occurs in the proteasome as well as the ESCRT-to-vacuole (lysosome) pathway. Cdc42p degradation at 37ºC promotes viability and proper cell polarity at the cost of mating sensitivity. At center (blue), Cdc42p can also be turned over by misfolding. The K16 residue is critical for Cdc42p stability, and K16R is not stable (Misfolding). Turnover of misfolded Cdc42p occurs in the proteasome, which if blocked leads to the formation of protein aggregates. Aggregates are confined in mother cells, which is an established way to prevent misfolded proteins from entering daughter cells (Rejuvenation). The regulation of turnover of mis-folded Cdc42p is presumably involved in a quality control mechanism surrounding the Cdc42p protein. At right, the active conformation of Cdc42p (red) is degraded by Ydj1p, Ssa1p and Rsp5p in the proteasome to attenuate the filamentous growth MAPK pathway (González and Cullen, 2022). TD refers to a turnover-defective version of Cdc42p lacking residues K5, K94, and K96.

MOVIES

Movie 1. Confocal time-lapse microscopy of the *cim3-1* mutant (PC5852) expressing GFP-Cdc42p (PC6454) on SD-URA media incubated at 37ºC. Cells were pre-incubated for 15 min at 37ºC before the analysis. Time interval, 10 min.

1295 **Movie 2.** Confocal time-lapse microscopy of the *cim3-1* mutant (PC5852) expressing GFP-
1296 Cdc42p^{K16R} (PC7697) on SD-URA media incubated at 37ºC. Cells were pre-incubated for 15 min
1297 at 37ºC before the analysis. Time interval, 10 min.